

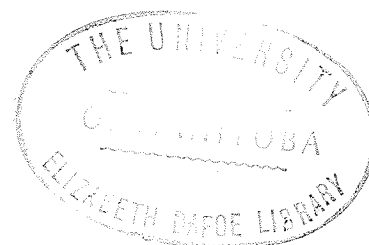
THE DEFORMATIONAL HISTORY OF A PORTION
OF THE OXFORD LAKE SUBGROUP,
GODS LAKE NARROWS, MANITOBA

A Thesis
Submitted to the
Faculty of Graduate Studies and Research
The University of Manitoba

In Partial Fulfillment
of the Requirements for the Degree
Master of Science

by
KARL O. GIESBRECHT

May, 1972



ABSTRACT

At Gods Lake Narrows, Manitoba, the Oxford Lake Subgroup has undergone a complex structural history involving several deformation events.

During the initial deformational event (D_1), large-scale isoclinal folds (f_1) involving bedding were produced by passive slip parallel to a well-developed axial planar penetrative foliation (s_1). The direction of tectonic transport was parallel to mineral lineations (m_1) and the long axes of deformed fragments (l_1) which plunge to the south in the plane of s_1 . The fragments (l_1) were also flattened in the plane of s_1 indicating relative shortening perpendicular to s_1 as well as extension of the rock mass parallel to s_1 .

The second deformational event (D_2) produced deformation of s_1 in the form of asymmetric z-shaped kink folds (f_2) which plunge west. Mineral lineations (m_2) and microcrenulations (c_2) are parallel to the fold axes. The folding mechanism was by flexural slip with an east-west component of shortening.

The third deformational event (D_3) produced horizontal symmetrical folds which deform s_1 and the axial planes of f_2 . The folding mechanism was by flexural slip

with a vertical component of shortening.

During the fourth deformational event (D_4) small asymmetric easterly-plunging z-shaped kink folds were produced. These deform s_1 but their relationship to f_2 and f_3 is not fully understood. Mineral lineations (m_4), microcrenulations (c_4), and the long axes of deformed fragments (l_4) are parallel to the fold axes. The folding mechanism was by flexural slip with an east-west component of shortening.

The fifth deformational event (D_5) was a period of small-scale faulting which displaces all earlier structures.

TABLE OF CONTENTS

	Page
ABSTRACT	iii
TABLE OF CONTENTS	v
LIST OF FIGURES	ix
LIST OF TABLES	xi
LIST OF MAPS	xii
 CHAPTER I - INTRODUCTION	 1
Statement of Problem	1
Location and Access	1
Previous Work	1
Present Work and Acknowledgements	3
 CHAPTER II - GENERAL GEOLOGY	 5
Introductory Statement	5
Gods Lake Subgroup	7
(1) Andesite and Basalt	7
(2) Quartz-Crystal Tuff	9
Oxford Lake Subgroup	9
(3a) Volcanic-Boulder Conglomerate	10
(3b) Hornblende Greywacke	11
(3c) Pillow Basalt	12
(3d) Basic Volcanic Breccia	13
(3e) Amphibolite	13
(3f) Garnetiferous Amphibolite	13
(3g) Fragmental Hornblende Greywacke	14
(3h) Iron Formation	14
(3i) Volcanic-Pebble Conglomerate	15

	<u>Page</u>
(3j) Acid Crystal Tuff	16
(3k) Paragneiss	16
Post-Oxford Intrusive Rocks	17
(4) Gneissic Granodiorite	17
(5) Gabbro	17
 CHAPTER III - EVIDENCE FOR POLYPHASE DEFORMATION	 19
The First Period of Deformation (D_1)	19
The Post D_1 Folding Events	20
The Second Folding Event (D_2)	20
The Third Folding Event (D_3)	22
The Fourth Folding Event (D_4)	22
Faulting (D_5)	24
 CHAPTER IV - STRUCTURAL GEOLOGY	 28
Structural Elements	28
Bedding (s_0)	28
Foliation (s_1)	28
Veins (s'_1)	30
Mineral Lineations (m_1, m_2, m_4)	32
Fragment Lineations (l_1, l_4)	32
Microcrenulations (c_2, c_4)	32
Boudinage (b_2)	34
Folds	34
Folds in Bedding (f_1, f'_1)	34
Folds in Foliation (f_2, f_3, f_4)	36
Faults	39
 CHAPTER V - THE FIRST DEFORMATIONAL EVENT	 42
Structural Elements Related to D_1	42
Geometric Analysis	42
Data	44
Discussion	44

	<u>Page</u>
Strain Analysis	47
Folding Mechanism	47
Tectonic Directions	48
CHAPTER VI - THE SECOND DEFORMATIONAL EVENT	49
Structural Elements Related to D_2	49
Geometric Analysis	49
Data	49
Discussion	50
Strain Analysis	50
Folding Mechanism	50
Tectonic Directions	53
Origin of Linear Structures	53
CHAPTER VII - THE THIRD DEFORMATIONAL EVENT	55
Structural Elements Related to D_3	55
Geometric Analysis	55
Strain Analysis	55
Folding Mechanism	55
Tectonic Directions	56
CHAPTER VIII - THE FOURTH DEFORMATIONAL EVENT	57
Structural Elements Related to D_4	57
Geometric Analysis	57
Data	57
Discussion	59
Strain Analysis	59
Folding Mechanism	59
Tectonic Directions	59
Origin of Linear Structures	61
CHAPTER IX - THE FIFTH DEFORMATIONAL EVENT	62

	<u>Page</u>
CHAPTER X - CONCLUSIONS	63
SELECTED REFERENCES	66

LIST OF FIGURES

	Page
Figure 1. Index map showing location of thesis area.	2
Figure 2. Locations of structural sub-areas.	21
Figure 3. Kink fold deforming the s_1 foliation.	21
Figure 4. f_2 kink fold refolded by f_3 symmetrical fold.	23
Figure 5. Late-stage faulting displacing crest of kink fold.	25
Figure 6. Chert interbedded with hornblende greywacke.	29
Figure 7. Bedding-foliation discordance in the volcanic-boulder conglomerate.	31
Figure 8. Foliation (s_1) and smaller incompetent fragments wrapping around large competent granitic fragments.	31
Figure 9. Aligned hornblende in the s_1 foliation plane.	33
Figure 10. Deformed fragments in the s_1 foliation plane.	33
Figure 11. Rotated boudins in a competent garnetiferous layer.	35
Figure 12. Shear folds developed in rocks where bedding and foliation are discordant.	35
Figure 13. Kink fold deforming bedding and s_1 foliation.	37
Figure 14. Kink fold deforming fragment flattened in s_1 .	37
Figure 15. Strain-slip cleavage displacing crest of f_2 kink folds.	38
Figure 16. f_2 kink fold with an axial planar quartz vein.	38
Figure 17. Shallowly-plunging f_3 symmetrical fold.	40

	Page
Figure 18. Graben-shaped structure produced by intersection of NNE and NNW-trending faults.	40
Figure 19. Displacement of bedding by late-stage faulting.	41
Figure 20. Cross-section A-B showing nature of f_1 isoclinal folding.	43
Figure 21. Lower hemisphere, equal-area stereogram of total map area; bedding (s_0).	45
Figure 22. Lower hemisphere, equal-area stereogram of total map area; foliation (s_1).	45
Figure 23. Lower hemisphere, equal-area stereogram of sub-area I; mineral lineations (m_1).	46
Figure 24. Lower hemisphere, equal-area stereogram of sub-area I; deformed fragments (l_1).	46
Figure 25. Lower hemisphere, equal-area stereogram of sub-area II; f_2 axial planes.	51
Figure 26. Lower hemisphere, equal-area stereogram of sub-area II; f_2 fold axes.	51
Figure 27. Lower hemisphere, equal-area stereogram of sub-area II; mineral lineations (m_2).	52
Figure 28. Lower hemisphere, equal-area stereogram of sub-area II; microcrenulations (c_2).	52
Figure 29. Lower hemisphere, equal-area stereogram of sub-area III; f_4 fold axes.	58
Figure 30. Lower hemisphere, equal-area stereogram of sub-area III; mineral lineations (m_4).	58
Figure 31. Lower hemisphere, equal-area stereogram of sub-area III; microcrenulations (c_4).	60
Figure 32. Lower hemisphere, equal-area stereogram of sub-area III; deformed fragments (l_4).	60

LIST OF TABLES

	Page
Table I Table of Formations	8
Table II Age Relationships of Structural Elements	26

LIST OF MAPS

	Page
Geology of the Gods Lake Narrows Area, Manitoba.	In Pocket

CHAPTER I

INTRODUCTION

Statement of Problem

The objective of this study is to determine the deformational history of part of the Oxford Lake Subgroup at Gods Lake Narrows, Manitoba. More specifically, the study deals with the character, geometry, and strain of each of several superimposed deformational events which have acted on these rocks.

Location and Access

The map area which is the subject of this study covers 65 square kilometres and is located approximately 600 kilometres northeast of Winnipeg, at Gods Lake Narrows, Manitoba (Fig. 1). The area is accessible by air travel; direct flights from Winnipeg to Gods Lake Narrows are available three times a week. Charter flights may also be arranged from Thompson and Ilford.

Previous Work

The first geological investigation of the area was conducted by Wright in 1931. His initial work resulted in

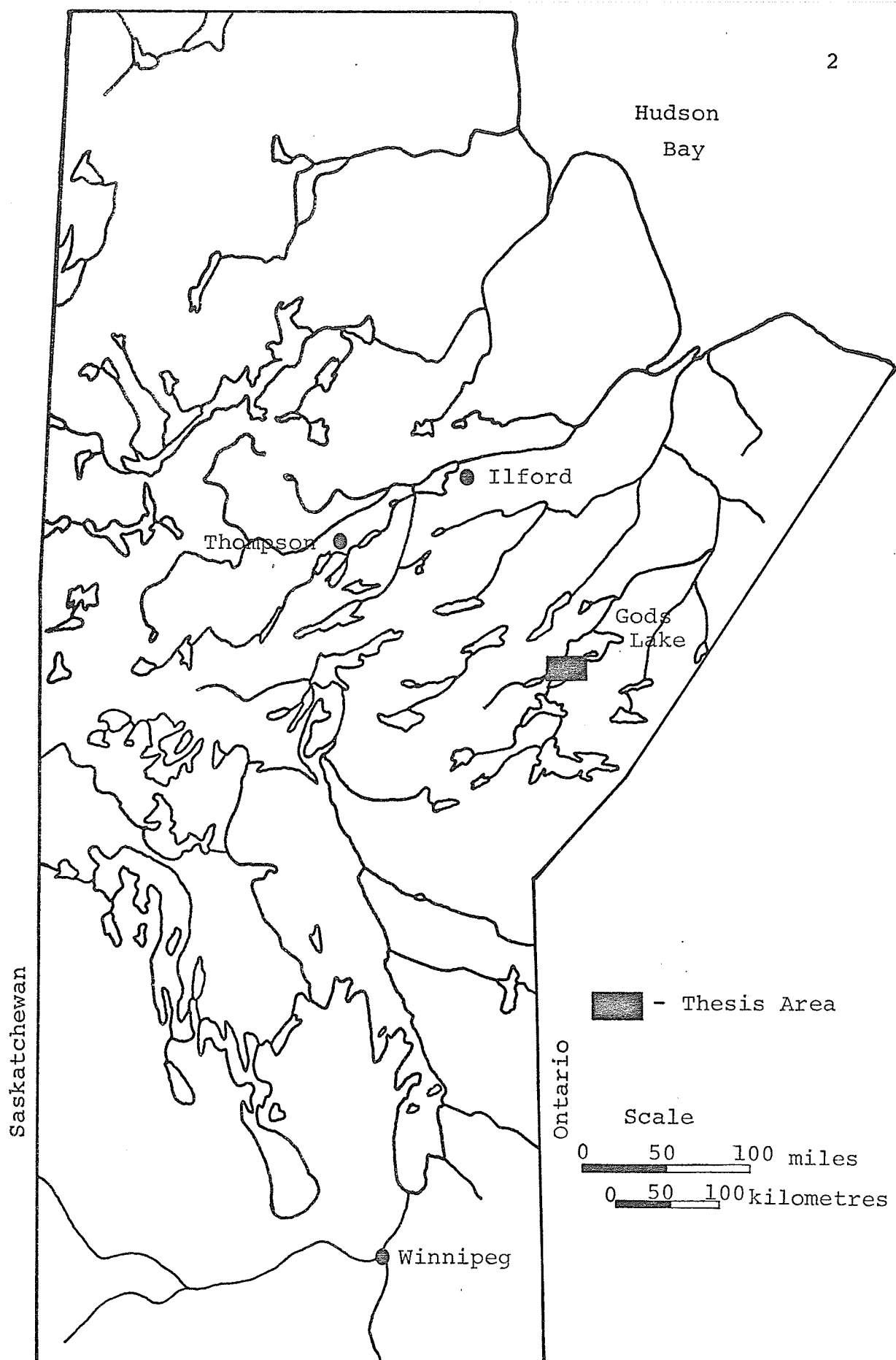


Figure 1. Index map showing location of thesis area.

a regional geological map of the Gods Lake-Oxford Lake area at a scale of 4 miles to the inch. Quinn (1956) mapped the area at a scale of 4 miles to the inch. In 1961, Barry mapped the Gods Lake Narrows area at a scale of 1 mile to the inch.

This earlier work served purely as a basis for an initial working hypothesis during the early phases of this study. The present study has led to a structural interpretation significantly different from earlier ones.

Present Work and Acknowledgements

This report embodies the results of six weeks of field work conducted during June and July, 1971. Shoreline mapping was carried out at a scale of $\frac{1}{4}$ mile to the inch using vertical aerial photographs for control. All outcrops exposed at the shorelines were examined. Inland traverses were not conducted because aerial photographs indicated that rock exposure covered less than one per cent of the total inland area.

Field mapping was carried out while employed by the Manitoba Department of Mines, Resources, and Environmental Management. Excellent advice and assistance were given by Dr. W.C. Brisbin (Professor and Geology, University of Manitoba) and Dr. F.H.A. Campbell (party chief). Much help was also received from B. Boyce, D. Fraser, and R. Hargreaves, all junior assistants from

the University of Manitoba.

CHAPTER II

GENERAL GEOLOGY

Introductory Statement

The map area is located in an easterly-trending greenstone belt within the northwestern part of the Superior Province of the Canadian Shield. The greenstone belt is approximately 15 kilometres wide at Gods Lake and contains two specific stratigraphic subdivisions, the Gods Lake Subgroup and the overlying Oxford Lake Subgroup which together form part of the Hayes River Group (terminology after Campbell, Elbers, and Gilbert, 1972). The Oxford Lake Subgroup, which is the object of this study, occupies the upper 5 kilometres of the sequence and is composed largely of volcanogenic metasedimentary rocks, as well as paragneiss, which is the uppermost unit of this subgroup. The Oxford Lake Subgroup is bounded to the north by a thick sequence of metamorphosed pillowed andesite, basalt, and minor quartz-crystal tuff belonging to the Gods Lake Subgroup. To the south, the Oxford Lake Subgroup grades from paragneiss into an unnamed series of orthogneisses and granitic intrusive rocks.

Structural relationships indicate the presence of a

non-conformable contact between the Gods Lake and Oxford Lake Subgroups. Metasedimentary rocks of the Oxford Lake Subgroup dip south and face south. Barry (1961) has mapped the older rocks of the Gods Lake Subgroup as dipping north and facing north and believes this to represent a major angular unconformity. Campbell (1972) has found no evidence of an angular unconformity but has mapped a mylonite between these two subgroups and suggests the possibility of a fault contact between them. The present study has indicated that Campbell's interpretation is probably correct.

Thin gabbro dykes intrude both the Gods Lake and Oxford Lake Subgroups. Gneissic granodiorite, in the north-western portion of the map area, contains possible inclusions of the Oxford Lake rocks. Both the gabbro and the gneissic granodiorite are interpreted as post-Oxford.

Rocks within the Oxford Lake Subgroup include: volcanic-boulder conglomerate, hornblende greywacke, pillowed basalt, fragmental hornblende greywacke, basic volcanic breccia, iron formation, amphibolite, garnetiferous amphibolite, volcanic-pebble conglomerate, acid crystal tuff, and paragneiss. Except for the volcanic-boulder conglomerate and the paragneiss, these rock types are extensively interbedded and can be separated only where one unit is predominant.

Bedding has an average strike of 115° and dips

range from 60° SW to 80° SW. The rocks all exhibit a well-developed penetrative foliation, most commonly parallel to the bedding.

This study has demonstrated that the rocks of the Oxford Lake Subgroup have undergone five deformational events, including one major period of folding, three minor periods of folding, and one period of faulting. Although indicator minerals are sparse the rocks are believed to have been metamorphosed to the upper greenschist or lower amphibolite facies.

The classification of rock units within the map area is given in the Table of Formations (Table I). Rock units 3b to 3j of the Oxford Lake Subgroup are extensively interbedded and are not necessarily in their correct chronological order. Each of the rock units presented in Table I is discussed in the following section. All ratios and dimensions presented in the following descriptions are in the horizontal plane unless stated otherwise.

Gods Lake Subgroup

(1) Andesite and Basalt

The andesite and basalt of the Gods Lake Subgroup outcrops in the northern part of the map area. Andesite is most commonly light green in color whereas basalt is black. Andesite usually contains greater than 50 per cent plagioclase and less than 50 per cent hornblende; basalt

TABLE I

TABLE OF FORMATIONS

RECENT AND
PLEISTOCENE

sand, gravel, silt, clay

UNCONFORMITY

Post-Oxford Intrusive Rocks

(5) gabbro

(4) gneissic granodiorite

P
R
E
C
A
M
B
R
I
A
N

INTRUSIVE CONTACT

Oxford Lake Subgroup

(3k) paragneiss

(3j) acid crystal tuff

(3i) volcanic-pebble conglomerate

(3h) iron formation

(3g) fragmental hornblende greywacke

(3f) garnetiferous amphibolite

(3e) amphibolite

(3d) basic volcanic breccia

(3c) pillow basalt

(3b) hornblende greywacke

(3a) volcanic-boulder conglomerate

FAULT CONTACT

Gods Lake Subgroup

(2) quartz-crystal tuff

(1)* undifferentiated, massive and
pillowed andesite and basalt

* Numbers in parentheses refer to map units
on accompanying geologic map.

usually contains less than 50 per cent plagioclase and greater than 50 per cent hornblende. These rocks are fine grained but display a weak foliation and form amphibolite schists where they have been sheared. The andesite and basalt flows may be both massive and pillowed. The pillows are either well formed or distorted. Pillows vary in size from 20 centimetres to one metre. The average size is 25 centimetres by 50 centimetres. At places the pillows are variolitic.

(2) Quartz-Crystal Tuff

Quartz-crystal tuff outcrops in the northern part of the map area and is interbedded with the volcanic flows of the Gods Lake Subgroup. Units range in thickness from one metre to one-half kilometre. In outcrop the quartz-crystal tuff is light grey in color. The quartz-crystal tuff is composed largely of quartz and feldspar with minor ferromagnesian minerals. The one characteristic common to all exposures of this rock type are large or small oval-shaped "eyes" of quartz. These quartz eyes stand up in relief and are commonly blue in color. This rock type is most commonly medium to coarse-grained and exhibits a definite fragmental texture.

Oxford Lake Subgroup

The metasedimentary rocks of the Oxford Lake

Subgroup are mapped on the basis of predominant lithology. Although the rock units are discussed in their approximate chronological order, this order is not necessarily correct because of extensive interbedding.

(3a) Volcanic-Boulder Conglomerate

This unit outcrops immediately south of the volcanic rocks of the Gods Lake Subgroup and is approximately 1,500 metres thick. It is the basal member of the Oxford Lake Subgroup.

The most distinctive feature of the conglomerate is the presence of ovoid boulders and cobbles of granitoid composition and texture. These boulders range in size from 2 centimetres to 70 centimetres and may comprise up to 20 per cent of the total rock. Granitoid fragments within the conglomerate include: quartz eye granite, various gneissic granitic rocks, diorite, and gabbro. Metavolcanic and metasedimentary fragments are also present in the conglomerate. These fragments are generally smaller than the granitoid fragments but are more numerous and may comprise up to 40 per cent of the total rock. Metavolcanic fragments include basalt, andesite, and porphyritic rhyolite. Metasedimentary fragments are iron formation, greywacke, and chert. Metavolcanic and metasedimentary fragments form flattened ellipsoids with length to width ratios of approximately 5:1. The metavolcanic, metasedi-

mentary, and some of the smaller granitoid fragments commonly wrap partially around the larger felsic clasts.

Beds of greywacke and subgreywacke are common within the conglomerate. These vary in thickness from 10 centimetres to 10 metres and average 45 centimetres. Individual beds may be correlated up to a maximum of 200 metres. Locally, graded beds provide good top determinations indicating tops to the south.

Clasts within the conglomerate unit are generally coarser at the base (north) and become finer towards the top (south), although this is not a regular progression and layers of larger clasts may be encountered anywhere within the unit. Similarly, the matrix at the base is generally amphibolitic, grading into greywacke or subgreywacke near the top.

(3b) Hornblende Greywacke

This unit is the most abundant rock type within the Oxford Lake Subgroup. The hornblende greywacke lies immediately above the volcanic-boulder conglomerate but is interbedded with most of the other Oxford metasedimentary rocks. The rock weathers from dark grey to black in color, depending upon the percentage of mafic minerals. The rock is composed of a fine-grained aggregate of hornblende and/or actinolite, biotite, plagioclase, quartz, and may also contain lesser amounts of potassium feldspar, muscovite,

chlorite, garnet, epidote, and magnetite. The hornblende greywacke is commonly well foliated, forming amphibole schists, but is also locally fine grained and massive. Bedding is well developed and individual beds have an average thickness of from 2 centimetres to 4 centimetres. Ferromagnesium minerals such as hornblende occupy up to 90 per cent of some beds. Interbedded light grey, fine-grained, cherty beds up to 5 centimetres thick are commonly drag folded. Graded bedding is most common in the lower part of this unit.

(3c) Pillow Basalt

Pillow basalt, belonging to the Oxford Lake Subgroup, occurs at two localities within the map area. One outcrop is on a small island in the eastern portion of the map area, just south of unit 3a; the second outcrop is on the second peninsula north of Gods Lake Narrows. The pillow basalt is interbedded with hornblende greywacke (3b) at both locations and is of limited extent. The rock weathers dark green to black in color. An average sample of this rock type is composed of hornblende, plagioclase, and epidote, with minor quartz, mica, chlorite, calcite, and magnetite. The rock is usually fine grained and a weak schistosity is common. The pillows have a maximum length of 75 centimetres and have been deformed with length to width ratios of approximately 4:1. Determinations of tops

from these pillows were not possible.

(3d) Basic Volcanic Breccia

One small occurrence of basic volcanic breccia, interbedded with hornblende greywacke, outcrops in the northwestern part of the map area. It weathers olive-green to black and both fragments and matrix have a basaltic composition. The fragments may be angular but are commonly elongated in the plane of the foliation. These fragments may attain a maximum length of 75 centimetres with length to width ratios of 7:1.

(3e) Amphibolite and (3f) Garnetiferous Amphibolite

Thin units of amphibolite and garnetiferous amphibolite occur approximately 2 kilometres north of Gods Lake Narrows. These units are up to 10 metres thick and have an average thickness of 3 metres. The rock weathers black and is only weakly schistose. Individual crystals are not aligned. Regular stratiform banding is locally present but not abundant.

The amphibole is usually hornblende and locally constitutes up to 90 per cent of the rock. Plagioclase is invariably more abundant than quartz. Several of these amphibolitic units contain almandine garnet up to 2 centimetres in diameter. These units are excellent marker horizons where the garnetiferous amphibolite (3f) is dominant.

(3g) Fragmental Hornblende Greywacke

Fragmental hornblende greywacke is located 2 kilometres north of Gods Lake Narrows and is interlayered with the hornblende greywacke. The units are up to 20 metres thick and average 10 metres. The rock weathers grey to black in color.

The fragmental hornblende greywacke is compositionally similar and gradational into the hornblende greywacke (3b). The fragmental hornblende greywacke is distinguished from the hornblende greywacke by the presence of fragments which vary from 10 centimetres to 50 centimetres in length and are elongated in the plane of the foliation. Length to width ratios of 8:1 are common. The fragments are compositionally similar to the matrix and can be distinguished on the weathered surface by slight variations in color. Because of the deformation that these rocks have suffered, it was not possible to determine whether the fragments were clastic or pyroclastic in origin.

(3h) Iron Formation

This unit outcrops $1\frac{1}{2}$ kilometres north of Gods Lake Narrows. Two varieties of iron formation occur at approximately the same stratigraphic level but are over 1 kilometre apart.

At the western most outcrop, the first type is nearly 3 metres thick and is composed of alternating beds

of chert and beds comprised of magnetite, hematite, and pyrite. These beds have an average thickness of 2 centimetres.

The second type outcrops in a 5 metre thick bed, and is massive and black. Fine-grained magnetite is the dominant constituent. No other iron oxides or sulphides are present.

Thin units of the second type are interbedded elsewhere with the hornblende greywacke. These were never more than 2 centimetres thick and could be distinguished only with a hand magnet.

(3j) Volcanic-Pebble Conglomerate

This unit outcrops 1 kilometre north of Gods Lake Narrows and is approximately 20 metres thick. It is characterized by a light brown color and by the presence of a small number of pink to grey granitoid fragments. Volcanic-derived fragments are dominant and constitute up to 60 per cent of the rock. The matrix and several interbeds up to 10 centimetres thick are greywacke or subgreywacke.

The granitoid fragments have an average length of 12 centimetres and are commonly elongated in the plane of the foliation. Length to width ratios average 4:1. Smaller volcanic-derived fragments have been more deformed and have length to width ratios up to 8:1. In many cases,

both types of fragments have been drag folded.

(3j) Acid Crystal Tuff

Acid crystal tuff outcrops at Gods Lake Narrows in units up to 150 metres thick. The rock weathers light grey. Thinner units are interbedded with the basic volcanic tuff. The larger units weather out as ridges up to 30 metres high.

The acid crystal tuff is characterized by feldspar crystals up to 4 centimetres in diameter in a fine to medium-grained groundmass. The crystals are commonly concentrated in zones and are locally fractured.

Bedding occurs locally in the finer-grained matrix. Because of its distinctive lithology, this unit served as a marker bed.

(3k) Paragneiss

Paragneiss is located immediately south of Gods Lake Narrows. It conformably overlies the pyroclastic and metasedimentary rocks to the north.

The paragneiss shows alternating grey and pink layers varying from 10 centimetres to 30 centimetres thick. These layers have a composition similar to that of greywacke and arkose respectively, however they have a good crystalline texture. Biotite and hornblende are commonly concentrated in layers up to 10 centimetres thick and are locally boudinaged. Small aplite and pegmatite dykes are common.

Post-Oxford Intrusive Rocks

(4) Gneissic Granodiorite

Gneissic granodiorite outcrops in the northwestern part of the map area, immediately north of the volcanic-boulder conglomerate. On both fresh and weathered surfaces, the rock is light to medium grey. An average sample of this rock type is composed of plagioclase, quartz, and biotite, with minor hornblende, magnetite, and epidote.

It is commonly medium grained but may be coarse grained where a few large pink feldspars are present. The penetrative foliation is caused by aligned hornblende and feldspar. The gneissic granodiorite commonly contains lenticular inclusions of biotite and hornblende schist which may be intricately folded and contorted. On the weathered surface these inclusions form depressions up to 3 centimetres deep. The gneissic granodiorite is intruded by pink medium-grained aplite dykes up to 2 metres wide.

(5) Gabbro

Gabbro locally intrudes Oxford Lake rocks, but its relationship to the gneissic granodiorite (4) is not known. The gabbro weathers black and has an average composition of 70 per cent hornblende, 25 per cent plagioclase, and 5 per cent quartz, with minor biotite, epidote, and calcite. The gabbro is coarse grained, except near the contact with Oxford Lake rocks, where it is fine to medium grained. In

a small shear zone the gabbro contains pyrrhotite and minor chalcopyrite.

CHAPTER III

EVIDENCE FOR POLYPHASE DEFORMATION

This chapter presents evidence for polyphase deformation in terms of the relative ages of folds, s-surfaces, and lineations. Identification of the relative ages of these structures is used, in turn, as a basis for the structural nomenclature.

The First Period of Deformation (D_1)

The first deformational event was a period of large scale isoclinal folding of the bedding. This folding event has been recognized from field evidence on the basis of top reversals and repetition of units. Several structural elements have been associated with this period of folding; these include small scale shear folds in the bedding, a penetrative axial planar foliation, quartz veins parallel to the foliation, lineation of minerals and long axes of deformed fragments in the plane of the foliation. Subsequent deformational events are recognized by deformation of the axial planar foliation developed during this earliest period of folding.

The Post-D₁ Folding Events

Several post-D₁ events have been interpreted because the geometry of the folds in the foliation is not consistent with a single pattern of strain.

For purposes of structural analysis, the map area was divided into three structural sub-areas (Fig. 2). Sub-area I is located in the northern portion of the area and contains only the volcanic-boulder conglomerate. Sub-area II is the largest and contains most of the rocks of the Oxford Lake Subgroup. Sub-area III is located in the southern portion of the area. The relative ages of several of these post-D₁ folding events is difficult to determine because of the restriction of some data to only one of these structural sub-areas.

The Second Folding Event (D₂)

The second period of deformation was a relatively minor period of kink folding. These kink folds are found mainly in sub-area II, are westerly plunging, have a z asymmetry, and deform the axial planar foliation developed during D₁ (Fig. 3). Structural elements associated with this second period of folding include: a strain-slip cleavage and quartz veins axial planar to the kink folds, lineation of minerals parallel to the plunge of the kink folds, microcrenulations parallel to the plunge of the kink folds, and rotated boudinage structure.

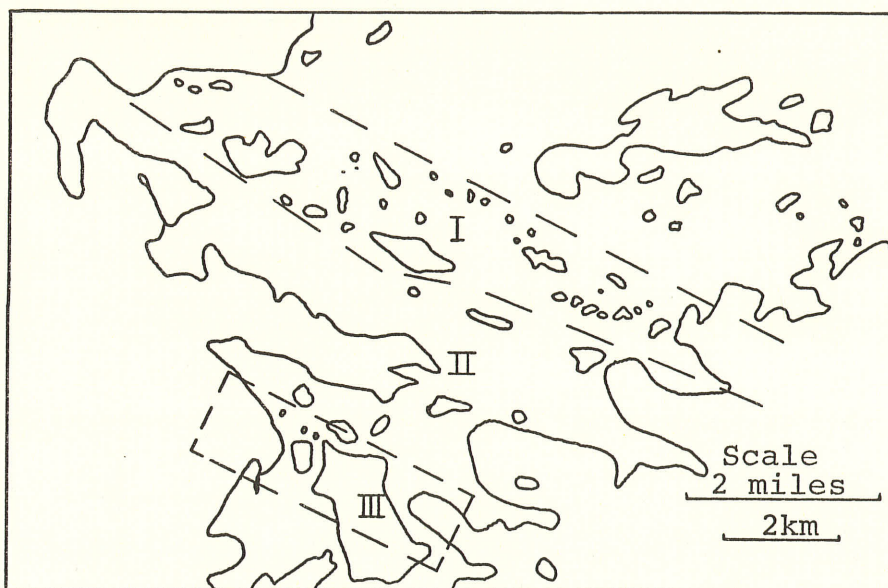


Figure 2. Locations of structural sub-areas.



Figure 3. Kink fold deforming the s_1 foliation.

The Third Folding Event (D_3)

The third period of deformation was a relatively minor period of symmetrical folding. These folds are located on the boundary between sub-areas II and III. These symmetrical folds deform the axial plane foliation developed during D_1 as well as the axial planes of the D_2 kink folds (Fig. 4).

The Fourth Folding Event (D_4)

The fourth deformational event was another relatively minor period of kink folding which is restricted to sub-area III. These kink folds are identical in character to the kink folds developed during D_2 , except for their easterly plunges. Structural elements associated with these easterly-plunging kink folds include lineations of minerals, aligned long axes of deformed fragments, and microcrenulations.

Because the structural elements associated with this fourth deformational event are restricted to sub-area III, the relative age and origin of this event is difficult to determine in relation to the other deformational events. However, in sub-area III there are a small number of poorly-developed westerly-plunging kink folds. These folds were possibly developed during D_2 and were then largely destroyed during subsequent periods of deformation. If this is true, the easterly-plunging kink folds were

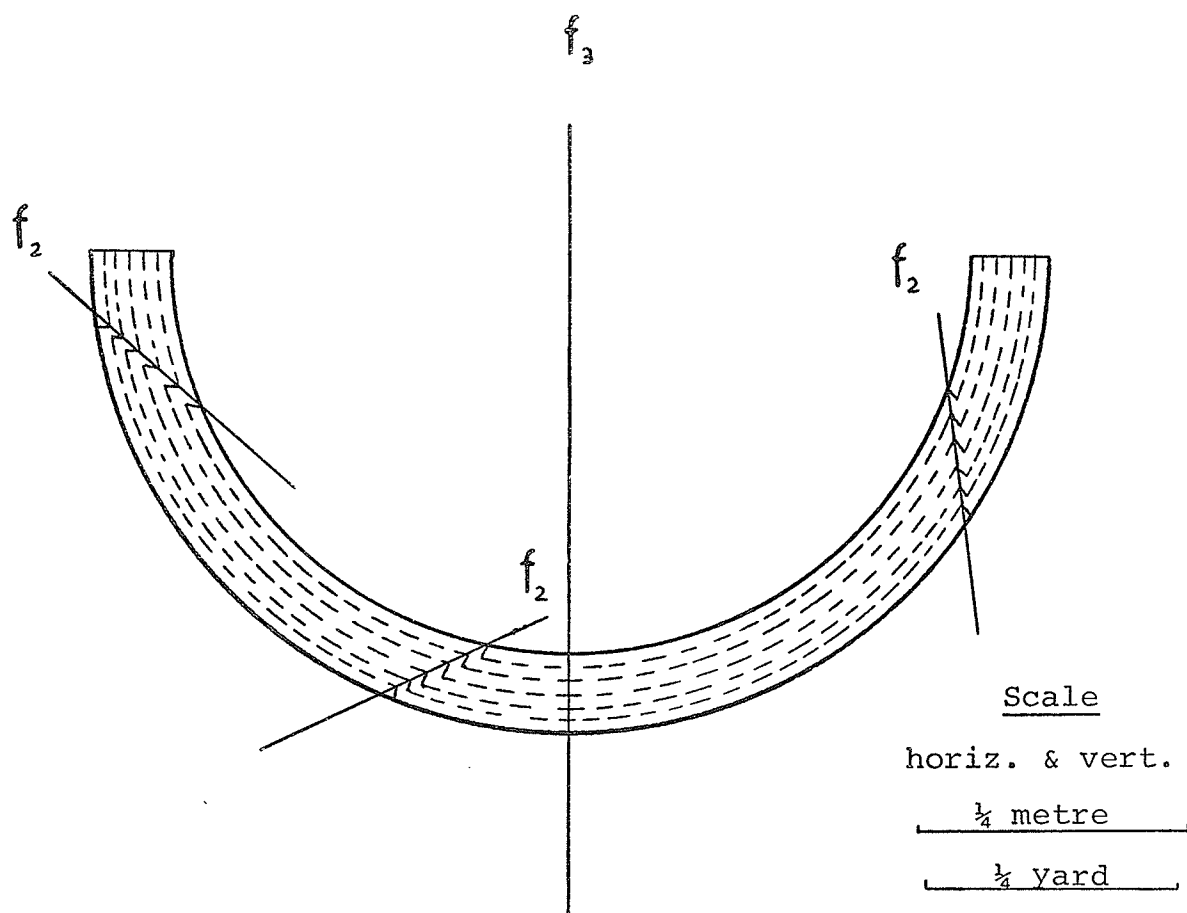


Figure 4. f_2 kink folds refolded by f_3 symmetrical fold.

developed after D_2 but their relationship to D_3 is not known.

Faulting (D_5)

The last deformational event was a minor period of faulting which displaces structures produced in all of the above deformational events. Figure 5 shows a kink fold displaced by a late-stage fault.

Table II summarizes the deformation events and the structural elements related to each event. In addition it presents the symbols used to label the various structural features.



Figure 5. Late-stage faulting displacing crest of kink fold.

TABLE II

AGE RELATIONSHIPS OF STRUCTURAL ELEMENTS

Deformational Event	Associated Structural Elements	Description
D_1	f_1, s_1, f_1'	f_1 - isoclinal folds of s_0
	s_1', l_1, m_1	s_1 - penetrative foliation axial planar to f_1 ; commonly parallel to s_0
		f_1' - shear folds developed in s_0 where s_1 is not parallel to bedding.
		s_1' - quartz veins, generally parallel to s_1
		l_1 - long axes of deformed fragments aligned in s_1
		m_1 - long axes of minerals aligned in s_1
D_2	f_2, s_2, s_2'	f_2 - kink folds with z asymmetry; plunge west; deform s_0, s_1, s_1' and l_1
	m_2, c_2, b_2	s_2 - strain-slip cleavage; axial planar to f_2 ; deforms f_2 crests
		s_2' - quartz veins; axial planar to f_2
		m_2 - long axes of minerals aligned parallel to f_2 axes.
		c_2 - microcrenulations parallel to f_2 axes; deforms s_0 and s_1
		b_2 - long axes of rotated boudins aligned in s_1

Table II (Continued)

Deformational Event	Associated Structural Elements	Description
D ₃	f ₃	f ₃ - horizontal symmetrical folds; deform s ₀ , s ₁ , and axial planes of f ₂
D ₄	f ₄ , m ₄ , c ₄ , l ₄	<p>f₄ - kink folds with z asymmetry; plunge east; deform s₀, s₁, and s₁</p> <p>m₄ - long axes of minerals aligned parallel to f₄ axes</p> <p>c₄ - microcrenulations parallel to f₄ axes; deforms s₀ and s₁</p> <p>l₄ - long axes of deformed fragments aligned parallel to f₄ axes</p>
D ₅	faulting	steeply-dipping faults trending NNE and NNW

CHAPTER IV

STRUCTURAL GEOLOGY

This chapter presents a description of the structural elements and diastrophic structures from the Gods Lake Narrows area. In some cases, different deformational events have produced structural elements which are identical except for their orientation. These structural elements will be described together.

Structural Elements

Bedding (s_0)

Bedding is preserved in all but the most highly-sheared rocks of the Oxford Lake Subgroup. Beds of fine-grained light-grey chert are abundant and conspicuous in the metasedimentary rocks. Figure 6 shows the typical form of this type of bedding. Beds composed of greywacke and subgreywacke occur within the conglomeratic units and may vary from 5 centimetres to 10 metres in thickness. Layers of feldspar crystals in the acid crystal tuff are utilized as bedding.

Foliation (s_1)

A well-developed penetrative foliation is present in

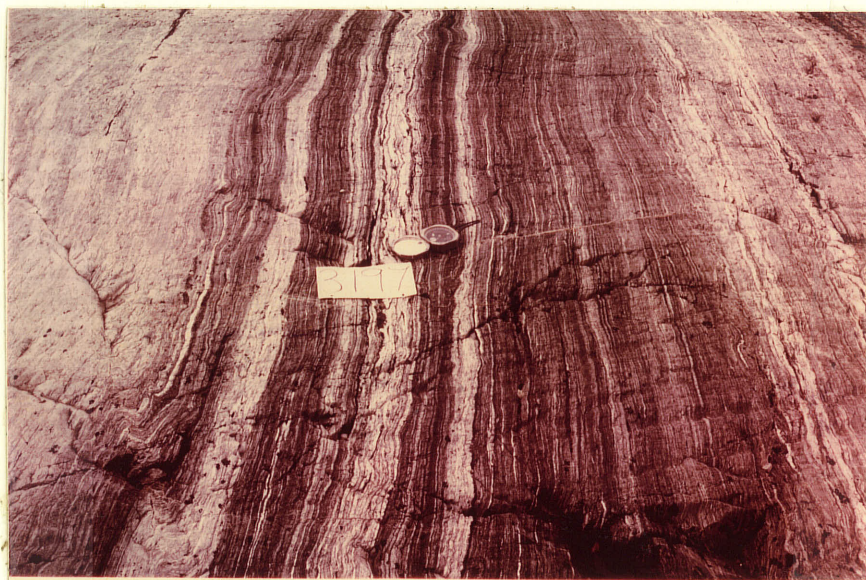


Figure 6. Chert interbedded with hornblende greywacke.

the rocks of the map area. The foliation is commonly parallel to the bedding (s_0), except in certain parts of the volcanic-boulder conglomerate (3a), where considerable discordances may exist (Fig. 7).

Volcanic and small granitic fragments within the conglomerate are commonly flattened in the plane of the foliation. The foliation and the flattened fragments are wrapped around the larger relatively undeformed granitic fragments (Fig. 8).

The s_1 foliation is best developed in the volcanic-boulder conglomerate and in the hornblende-rich meta-sedimentary rocks. In both hand specimen and thin section the foliation results from the planar preferred orientation of hornblende. Detrital quartz and feldspar are slightly rounded and locally show evidence of crushing.

Several shear zones are recognized within the map area. These are parallel to the s_1 foliation. Rocks from these shear zones exhibit an extremely fine-grained mylonitic texture.

Veins (s'_1)

Quartz veins are commonly parallel to the bedding (s_0) and foliation (s_1), although some are oblique to these surfaces. They vary in thickness from 2.5 millimetres to 30 centimetres, pinch, swell, and are often discontinuous.

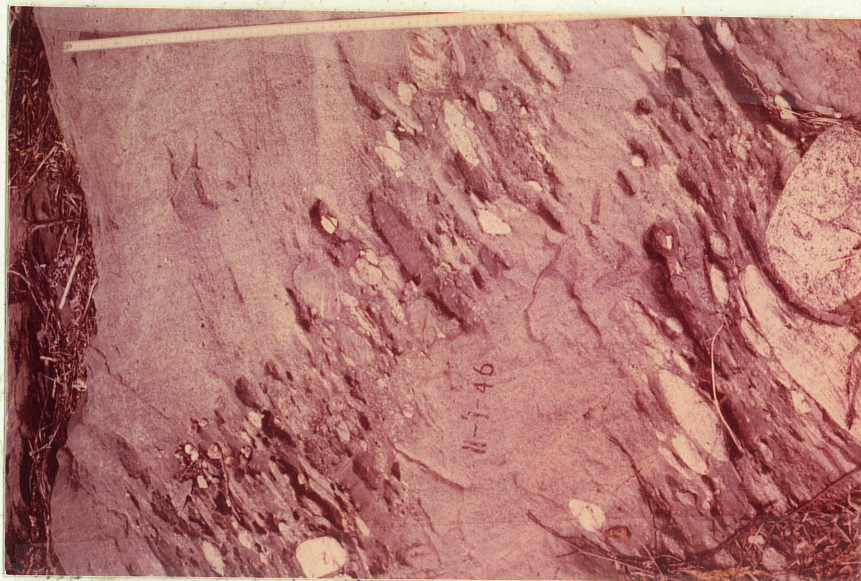


Figure 7. Bedding-foliation discordance in the volcanic-boulder conglomerate.



Figure 8. Foliation (s_1) and smaller incompetent fragments wrapping around large competent granitic fragments.

Mineral Lineations (m_1, m_2, m_4)

Mineral lineations have been produced during three separate deformational events and are identical except for their attitude. These mineral lineations most commonly are a result of a linear orientation of hornblende in the plane of the foliation (Fig. 9).

Fragment Lineations (l_1, l_4)

Fragment lineations have been developed during two separate deformational events and are identical except for their orientation. The long axes of deformed fragments are aligned in the volcanic-boulder conglomerate (3a) and the volcanic-pebble conglomerate (3i). The volcanic fragments and small felsic fragments are commonly deformed as tri-axial ellipsoids with axial ratios of 6:3:1 (Fig. 10). The long and intermediate axes of these fragments lie in the plane of the foliation. Measurements of the attitudes of these fragments were difficult to make because of weathering. Nevertheless, it appears that the attitude of the long axes of the deformed fragments and the attitude of the mineral lineations are nearly coincident.

Microcrenulations (c_2, c_4)

Microcrenulations have been produced during two deformational events and are distinguishable only by their attitude. They are found throughout the metasedimentary rocks in the area and deform the bedding (s_0) and the

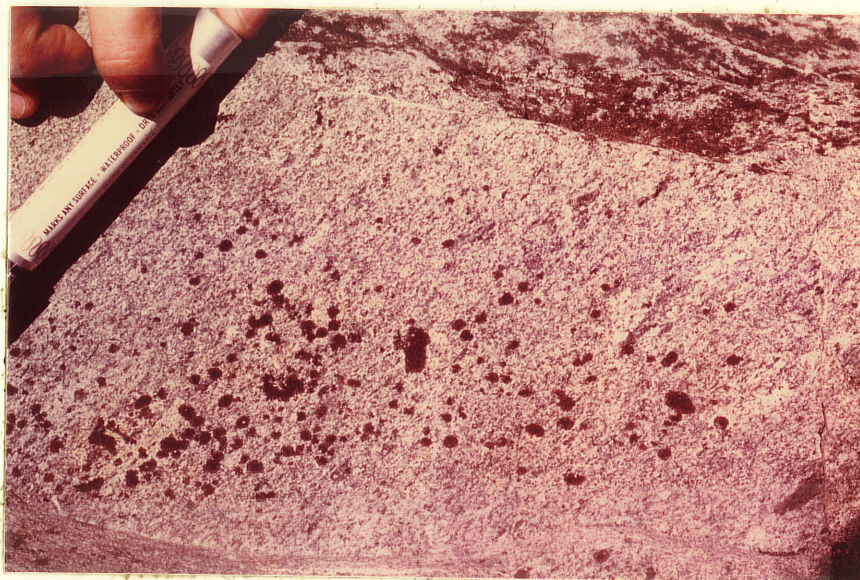


Figure 9. Aligned hornblende in the s_1 foliation plane.



Figure 10. Deformed fragments in the s_1 foliation plane.

foliation (s_1).

Boudinage (b_2)

Boudinage structure in the hornblende greywacke (3b) is characterized by the attenuation, and commonly the separation of a competent garnetiferous layer. Individual boudins are often rotated with respect to the surrounding rock (Fig. 11). The less-competent surrounding metasedimentary rocks have undergone concomitant flow into the "neck zones" where recrystallized quartz is also common.

Folds

Folds in Bedding (f_1, f'_1)

The metasedimentary rocks of the Oxford Lake Subgroup have been folded into a series of overturned, shallowly-plunging isoclinal folds (f_1). Axial planes have an attitude of $120^\circ/60^\circ$ SW, parallel to the dominant bedding and foliation directions. Although no closures were identified, four axial planes have been defined on the basis of top determinations from graded beds and from the repetition of units. The attitudes of the limbs of these folds differ by only a few degrees throughout the sequence.

Shear folding (f'_1) locally occurs in chert, amphibolite, and hornblende greywacke, where bedding and foliation are discordant (Fig. 12). Bedding has been folded by passive slip along foliation planes.

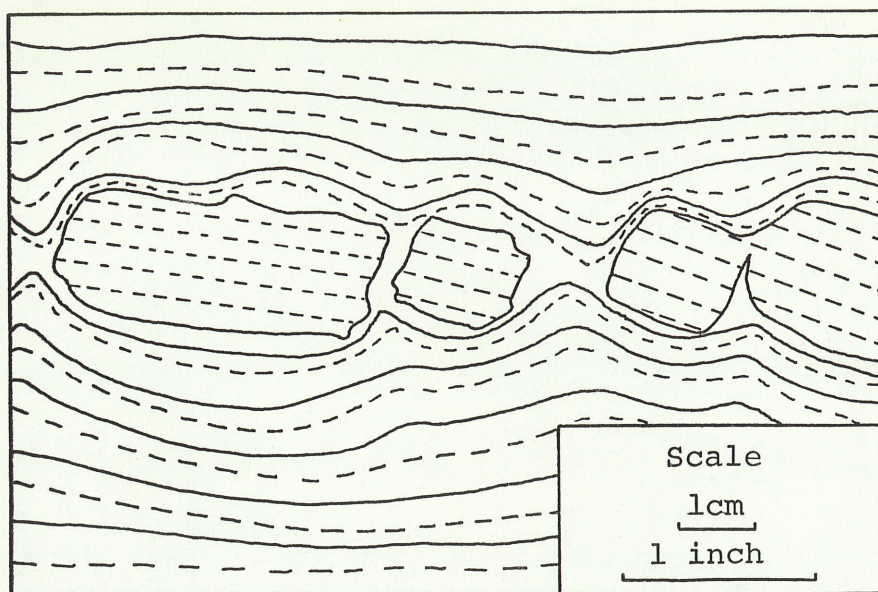


Figure 11. Rotated boudins in a competent garnetiferous layer.

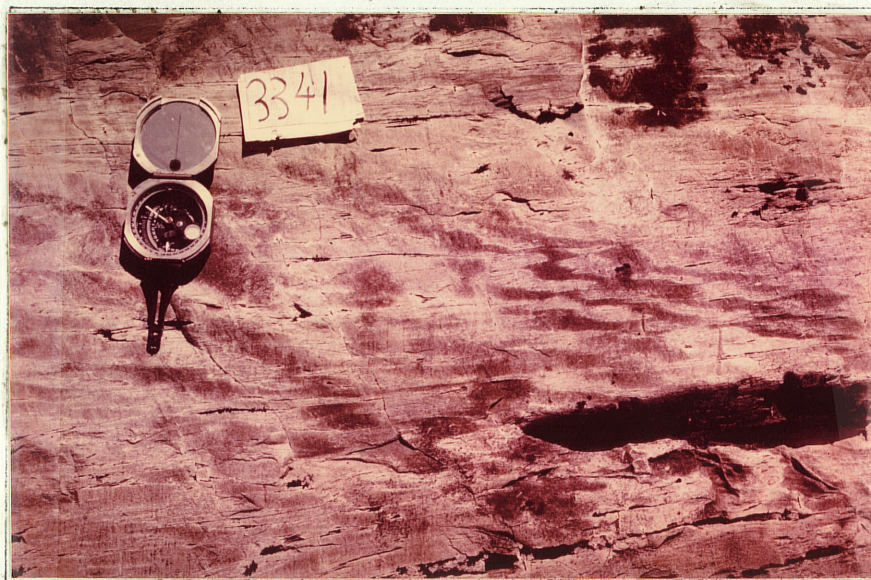


Figure 12. Shear folds developed in rocks where bedding and foliation are discordant.

Folds in Foliation (f_2, f_3, f_4)

Small folds are common in the foliated metasedimentary rocks of the Oxford Lake Subgroup. These folds are grouped into three major categories: (1) asymmetrical z-shaped westerly-plunging kink folds (f_2), (2) asymmetrical z-shaped easterly-plunging kink folds (f_4), and (3) symmetrical non-plunging folds (f_3).

The first two are identical in character except for the orientation of their axes. The kink folds deform bedding (s_0), quartz veins (s_1'), foliation (s_1), and elongated clasts flattened in the plane of the s_1 foliation (l_1, l_4), (Figs. 13, 14). Strain-slip cleavage (s_2) is commonly associated with the kink folds, and may deform the fold crests (Fig. 15). Axial planar quartz veins (s_2') are locally present in the kink folds (Fig. 16).

Although the kink folds are not true kink bands, they have a definite chevron style. The kink folds average 10 cm in relief although exceptionally large kink folds up to one and one half metres have been noted. The closure is commonly between 45° and 90° , and limb ratios are generally greater than 10:1. Right sections of these folds have a concentric style with axial planes bisecting the interlimb angle. These kink folds have a z asymmetry when plotted in plan view.

The third type, symmetrical folds (f_3), occur in a local area one kilometre north of Gods Lake Narrows. These folds



Figure 13. Kink fold deforming bedding and s_1 foliation.



Figure 14. Kink fold deforming fragment flattened in s_1 .



Figure 15. Strain-slip cleavage displacing crests of f_2 kink folds.

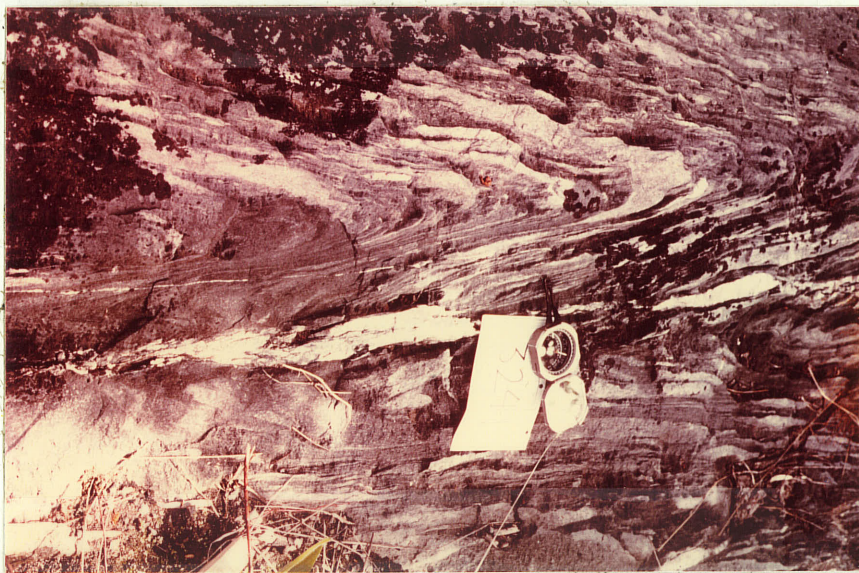


Figure 16. f_2 kink fold with an axial planar quartz vein.

deform bedding (s_0), foliation (s_1), and the axial planes of f_2 . The folds plunge very shallowly or are horizontal, with near-vertical axial planes. Closure commonly ranges from 90° to 150° , and the folds show a relief of up to several metres (Fig. 17).

Faults

Minor faults are common throughout the map area. They are best developed in the more competent units such as acid crystal tuff and chert. Displacement along fault surfaces is never more than 20 centimetres. Figure 18 shows a graben-shaped structure produced by the intersection of two faults with different orientations but with the same relative movements. Figure 19 shows displacement of bedding and foliation by faulting.

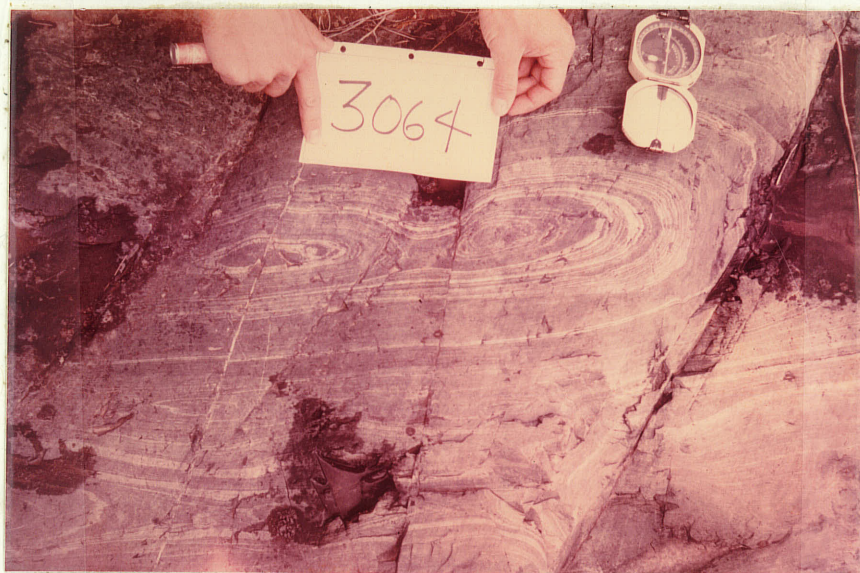


Figure 17. Shallowly-plunging f_3 symmetrical fold, brassiere shape is produced by erosion.



Figure 18. Graben-shaped structure produced by intersection of NNE and NNW-trending faults.



Figure 19. Displacement of bedding by late-stage faulting.

CHAPTER V

THE FIRST DEFORMATIONAL EVENT

Structural Elements Related to D_1

The first generation of folds (f_1) are large-scale and isoclinal in character. They have been interpreted on the basis of top reversals and repetition of units. Figure 20 is a cross-section through the Oxford Lake Subgroup showing the nature of this folding event. Several structural elements are associated with this period of folding. A strong penetrative foliation (s_1) developed parallel to the axial planes of the isoclinal folds. Deformed fragments (l_1) and mineral lineations (m_1) are developed in the plane of the foliation. Where bedding (s_0) and foliation (s_1) are locally discordant small-scale shear folds (f'_1) are present.

Geometric Analysis

In the analysis of the structural elements developed during D_1 , it was necessary to deal with the total map area. Although all data collected in the field was plotted this is probably still not a true statistical average.

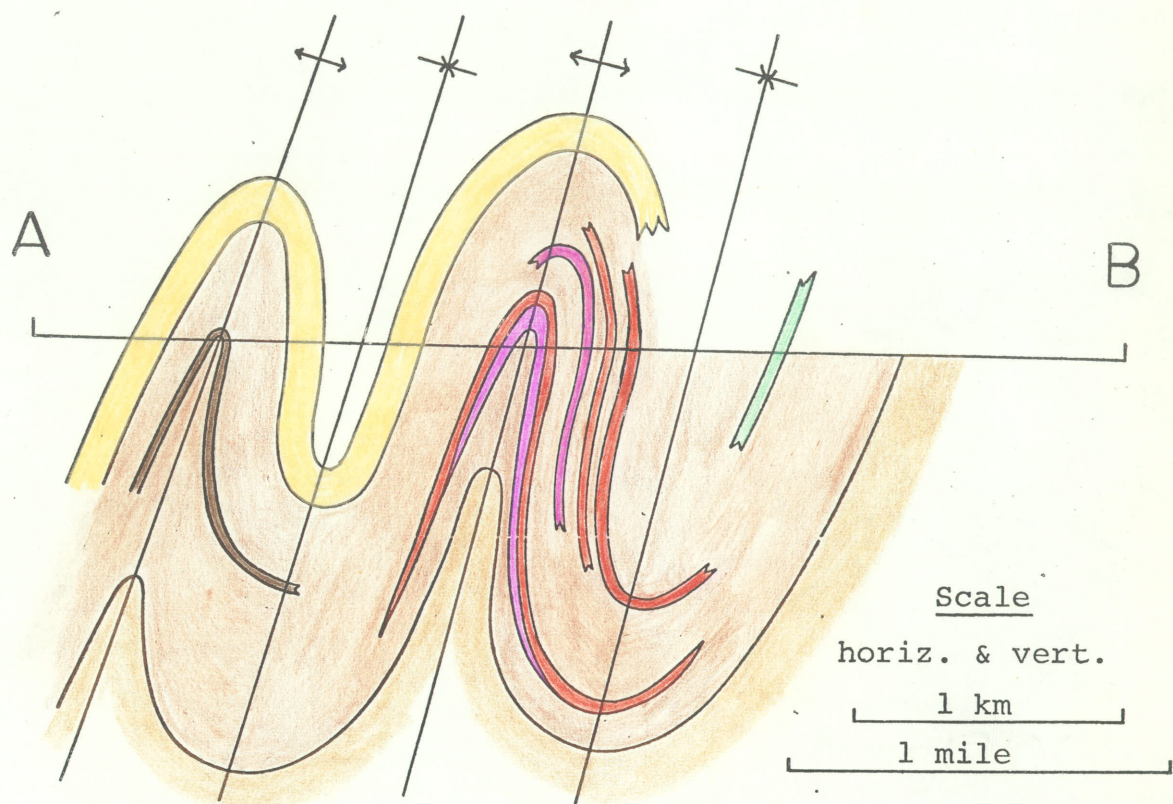


Figure 20. Geologic cross-section A-B showing nature of isoclinal folding.

- Acid crystal tuff
- Volcanic-pebble conglomerate
- Garnetiferous amphibolite
- Fragmental hornblende greywacke
- Hornblende greywacke
- Pillow basalt
- Volcanic-boulder conglomerate

Data

Poles to bedding (s_0) from the entire map area show a single concentration striking 115° and dipping 65° SW (Fig. 21). A plot of poles to foliation from the entire map area show a single concentration striking 115° and dipping 65° SW (Fig. 22). Mineral lineations plotted from sub-area I show a single concentration which plunges 65° in a direction 185° (Fig. 23). Mineral lineations from sub-areas II and III were not plotted as they are believed to have been affected by further deformational events. A plot of the long axes of deformed fragments show two closely spaced concentrations which have attitudes of $60^\circ/205^\circ$ and $60^\circ/195^\circ$ (Fig. 24). For all practical purposes these are considered to be parallel to the mineral lineations (m_1).

Discussion

Poles to bedding (s_0) which include both normal and overturned beds show a single concentration. Axial planes are parallel to bedding. A penetrative foliation lies in the axial plane of these folds; the foliation is a result of recrystallization and is consequently interpreted to have developed synchronously with the folding. Similarly, both mineral lineations (m_1) and the long axes of deformed fragments (l_1) lie in the foliation plane and were probably developed during this event.



Figure 21. Lower hemisphere, equal-area stereogram of total map area; bedding (s_0), 193 poles, contours 1%, 9%, 17%.



Figure 22. Lower hemisphere, equal-area stereogram of total map area; foliation (s_1), 230 poles, contours 1%, 5%, 13%.

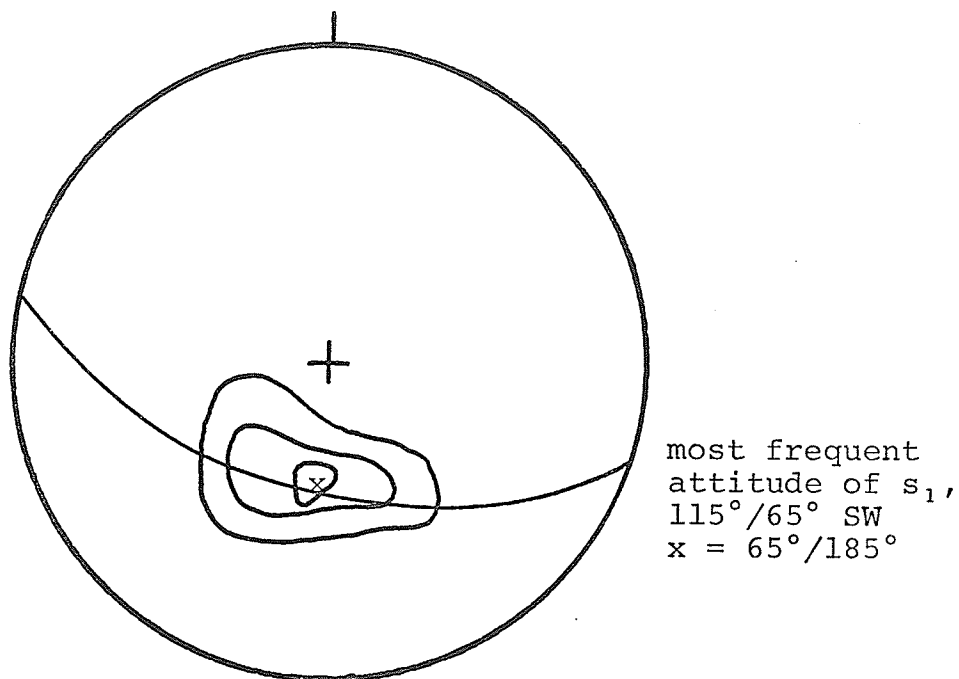


Figure 23. Lower hemisphere, equal-area stereogram of sub-area I. Mineral lineations (m_1), 37 points, contours 6%, 18%, 24%.

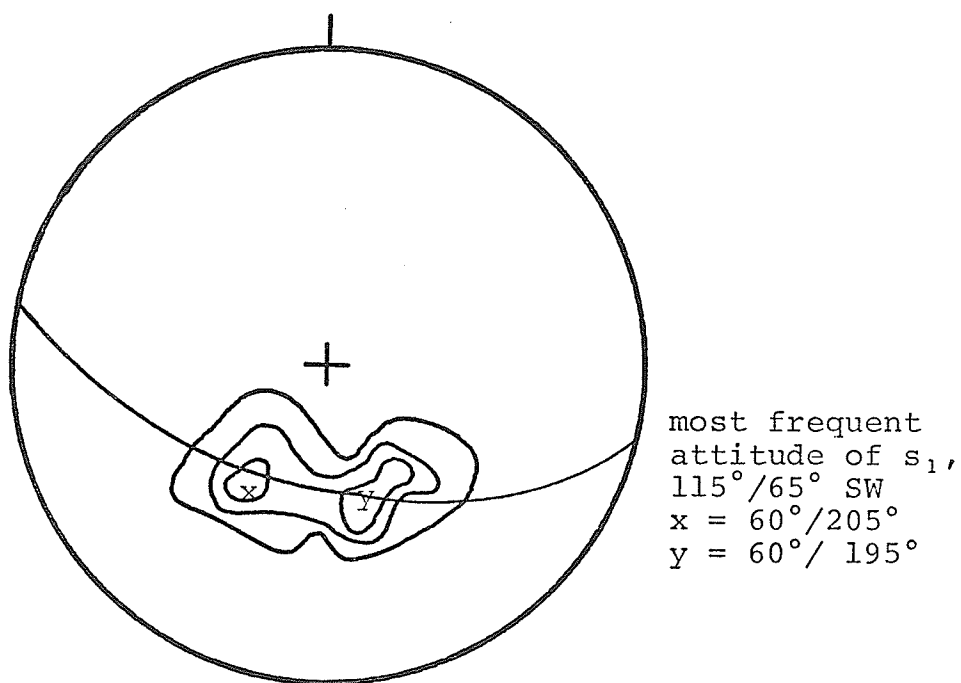


Figure 24. Lower hemisphere, equal-area stereogram of sub-area I. Long axes of deformed fragments (l_1), 33 points, contours 8%, 15%, 21%.

Strain Analysis

Folding Mechanism

Considerable evidence is present to suggest that the first generation fold mechanism was passive slip produced by differential pure shear. Deformation by passive slip is defined by Donath and Parker (1964) as macroscopically visible slip crossing the boundaries of layers which exercise little or no control over their own deformation. Pure shear is described by Hills (1963) as follows:

"a strain in which the extension along one principle axis is so related to the shortening on the other that an inscribed rhombus becomes after deformation a congruent rhombus, the obtuse and the acute angles being interchanged".

Evidence in support of this type of deformation is summarized below:

1. The development of a widespread penetrative foliation.
2. Small shear folds (f'_1) formed by discrete displacements along a penetrative foliation (s_1) suggests that the isoclinal folds (f_1) were also deformed passively.
3. The axial planes of the isoclinal folds (f_1) have the same orientation as the penetrative foliation (s_1).
4. Fragments are flattened in the plane of the foliation suggesting that a major portion of the strain was compression perpendicular to the axial

planes of the isoclinal folds. This is consistent with the orientation of a recrystallization type of foliation.

5. Mineral lineations (m_1) and deformed fragments (l_1) are parallel to each other. The orientation of the long dimension is parallel to the dip of the f_1 axial planes. This suggests that the rocks have in fact undergone pure shear rather than simple shear and also that a significant portion of the strain was extension parallel to these linear structures. Differential amounts of extension with this orientation would be consistent with the shallowly plunging folds which have been interpreted to have developed during D_1 . The degree to which simple shear may have taken place on the s_1 anisotropy developed by pure shear is not known.

Tectonic Directions

The identification of passive slip on s_1 suggests that s_1 is the kinematic a-b plane of movement which produced folds during the first period of deformation. The apparent direction of tectonic transport, the kinematic a direction, is parallel to the mineral lineations (m_1) and the deformed fragments (l_1) which lie in the plane of the foliation (s_1).

CHAPTER VI

THE SECOND DEFORMATIONAL EVENT

Structural Elements Related to D_2

The second deformational event was relatively minor and resulted in the development of small-scale westerly-plunging kink folds which are particularly well developed in sub-area II. These kink folds are best-developed in the less competent, well-foliated, metasedimentary rocks. The folds deform bedding (s_0), foliation (s_1), and quartz veins (s_1'). Mineral lineations (m_2) and microcrenulations (c_2), which are the small-scale equivalents of the f_2 folds, parallel the axes of the f_2 folds. A late strain-slip cleavage (s_2) parallel to the f_2 axial planes deforms the f_2 crests. Axial planar quartz veins (s_2') are also locally present.

Geometric Analysis

The geometric analysis of the second deformational event incorporates data dominantly from sub-area II.

Data

A plot of poles to axial planes of the f_2 folds shows

a major concentration striking at 100° and dipping 70° to the south (Fig. 25). These are at an angle of approximately 15° to the bedding (s_0) and foliation (s_1) directions. A plot of f_2 fold axes shows a single concentration at $35^\circ/270^\circ$ (Fig. 26). Mineral lineations (m_2) plot with a single concentration at $35^\circ/270^\circ$ (Fig. 27). This is identical with the plunge of the minor fold axes. Although insufficient data was available for a statistical plot of the microcrenulations, eleven measurements suggest that they have an attitude similar to that of both the fold axes and the mineral lineations (Fig. 28).

Discussion

The consistent orientation of the minor fold axes and the identical orientation of mineral lineations (m_2) and microcrenulations (c_2) suggest that these were formed during the same deformational event as the f_2 folds.

Strain Analysis

Folding Mechanism

There is considerable evidence which suggests that the second period of folding was produced by flexural slip on the s_1 foliation. This mechanism is described by Donath and Parker (1964) as slip restricted by layer boundaries which exercise an active control over their own deformation. In sub-area II the kink folds in bedding

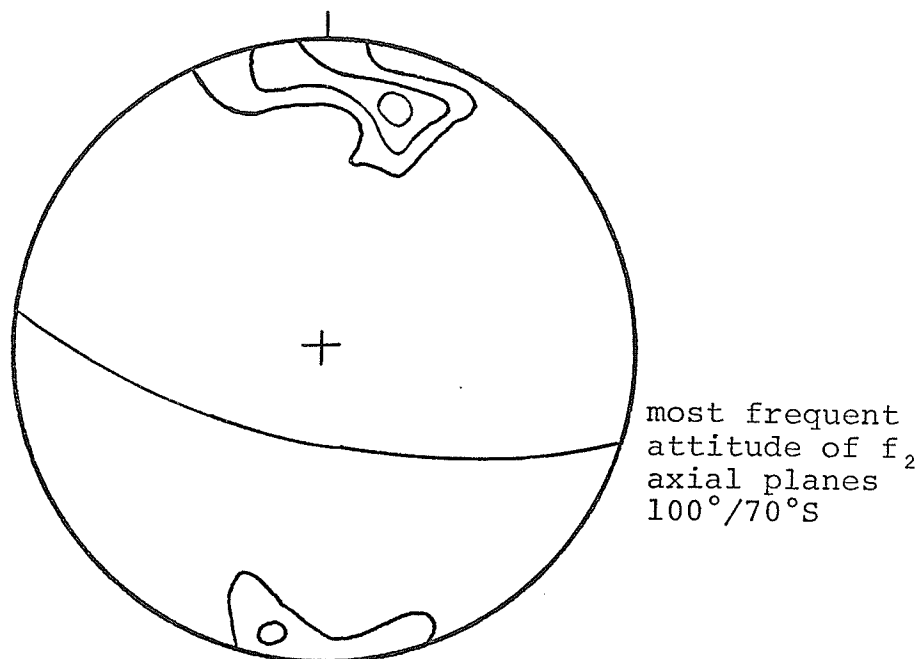


Figure 25. Lower hemisphere, equal-area stereogram of sub-area II. f_2 axial planes, 48 poles, contours 4%, 7%, 13%.

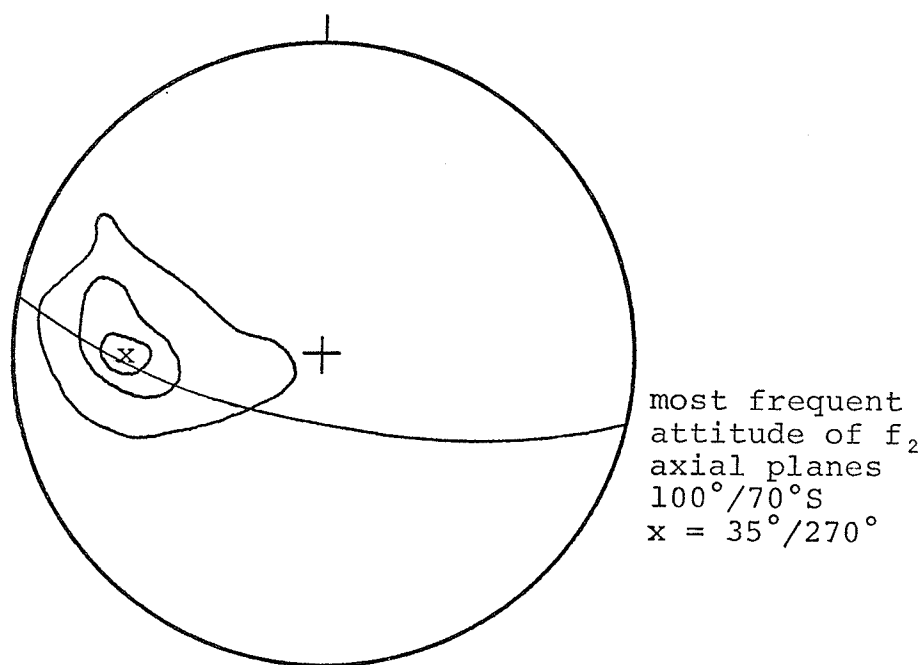


Figure 26. Lower hemisphere, equal-area stereogram of sub-area II. Fold axes (f_2), 66 points, contours 3%, 11%, 20%.

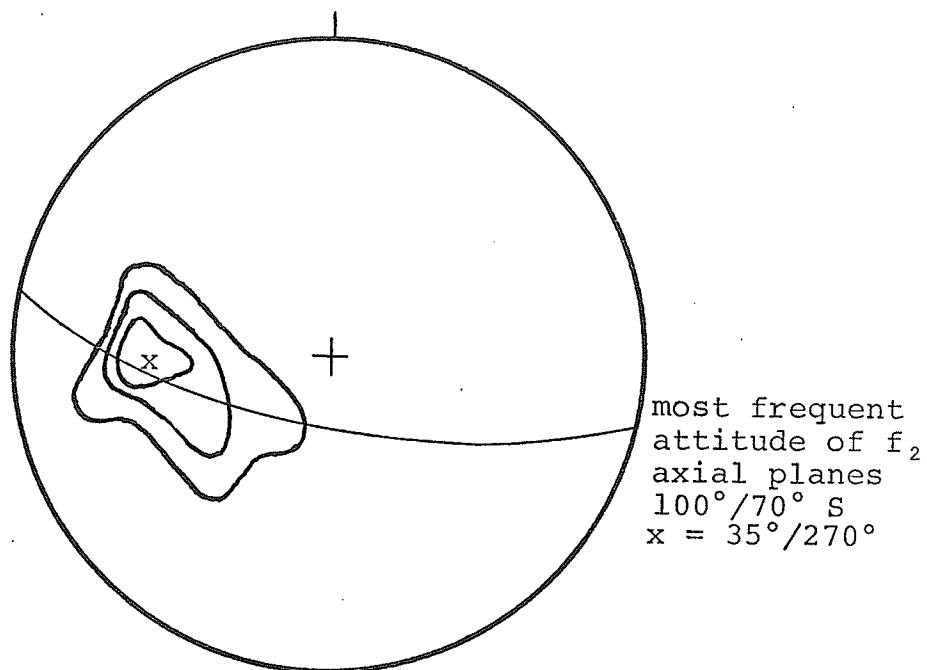


Figure 27. Lower hemisphere, equal-area stereogram of sub-area II. Mineral lineations (m_2), 41 points, contours 3%, 8%, 15%.

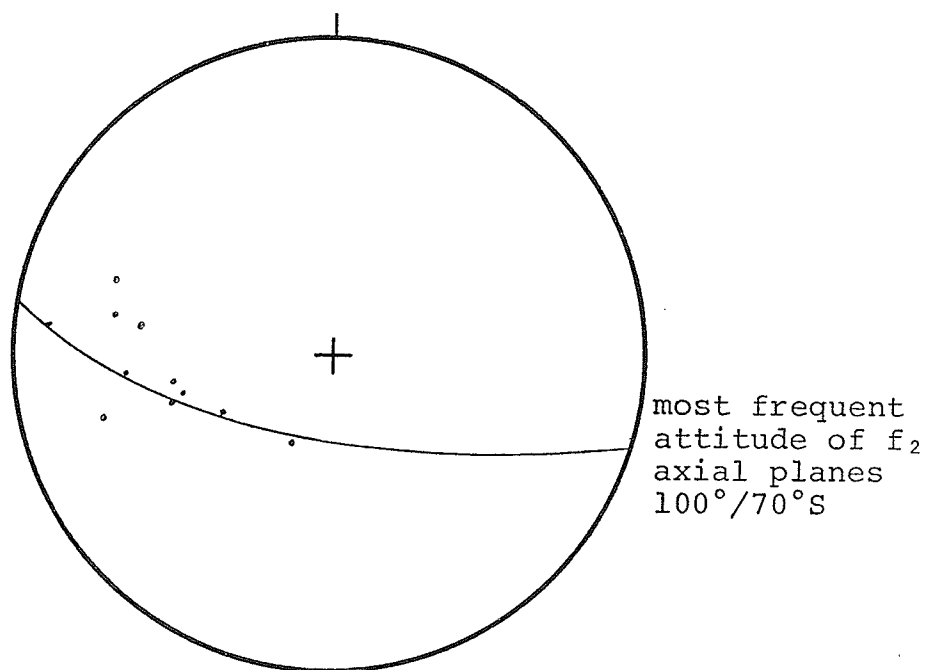


Figure 28. Lower hemisphere, equal-area stereogram of sub-area II. Microcrenulations (c_2), 11 points.

(s_0), foliation (s_1), and quartz veins (s_1) are interpreted to have formed by flexural slip because of the following evidence:

1. In right sections the layer thickness between successive foliation planes remains constant.
2. Axial planes bisect the interlimb angle.
3. Both mineral lineations and microcrenulations are parallel to the statistical fold axes in sub-area II.
4. The s_1 foliation forms an ideal anisotropy for flexural folding and changes attitude around the nose of the folds.

Tectonic Directions

Both the kinematic b direction and the a - c plane can be defined for flexural slip folding. The b direction is parallel to the fold axes. By definition, the a - c plane of deformation is perpendicular to the b direction. The a - c plane therefore strikes due north and dips 55° to the east. The direction of tectonic transport, or the kinematic a direction will vary in the a - c plane according to the attitude of the limbs on various parts of the fold. The orientation of the kink folds suggests an east-west component of shortening perpendicular to the f_2 plunge direction.

Origin of Linear Structures

Both microcrenulations (c_2) and mineral lineations

(m_2) are parallel to the f_2 statistical fold axis in sub-area II. The microcrenulations (c_2) are the small-scale equivalents of the f_2 kink folds. The origin of the mineral lineations (m_2) however, is not fully understood. They may represent an earlier lineation reoriented during D_2 , or the development of a new lineation by recrystallization during D_2 . The latter interpretation appears more probable because of the well established coincidence between the orientation of the m_2 lineations and the orientation of the f_2 fold axes.

CHAPTER VII

THE THIRD DEFORMATIONAL EVENT

Structural Elements Related to D_3

The third deformational event is expressed by local symmetrical folds. These folds differ from the f_2 folds on the basis of their style, symmetry, and their horizontal plunge. The folds deform bedding (s_0), foliation (s_1), quartz veins (s_1'), and the f_2 axial planes (Fig. 4).

Geometric Analysis

The limited number of folds within the map area prevents a statistical analysis of the f_3 folds. The f_3 axial planes strike at 105° and are approximately vertical. The fold axes are horizontal.

Strain Analysis

Folding Mechanism

The following evidence suggests that the f_3 folds were produced by flexural slip:

1. The layer thickness remains constant in right sections.

2. Axial planes bisect the interlimb angle.

Tectonic Directions

In flexural slip folding, the b kinematic direction is defined as parallel to the f_3 fold axes. The a-c plane of deformation is perpendicular to the b direction striking at 195° , and is vertical. The direction of tectonic transport kinematic a, will vary in the a-c plane according to the attitudes of the fold limbs. The geometry of these f_3 folds suggests a major component of shortening in a vertical direction perpendicular to the f_3 plunge direction.

CHAPTER VIII

THE FOURTH DEFORMATIONAL EVENT

Structural Elements Related to D_4

The fourth deformational event is defined by kink folds (f_4). These folds are best developed in sub-area III, and are identical to f_2 folds except for their direction of plunge, which is east. The kink folds deform s_0 , s_1 , and s_1' . Linear structures associated with this period of folding include mineral lineations (m_4), microcrenulations (c_4) and deformed fragments (l_4).

Geometric Analysis

The geometric analysis of the fourth deformational event involves data from sub-area III.

Data

A plot of fold axes from sub-area III shows a major concentration at $40^\circ/110^\circ$. A minor concentration has an attitude of $55^\circ/265^\circ$ (Fig. 29). Although insufficient data was available to plot mineral lineations (m_4), microcrenulations (c_4), and deformed fragments (l_4) statistically, the available data suggests a good correlation between the

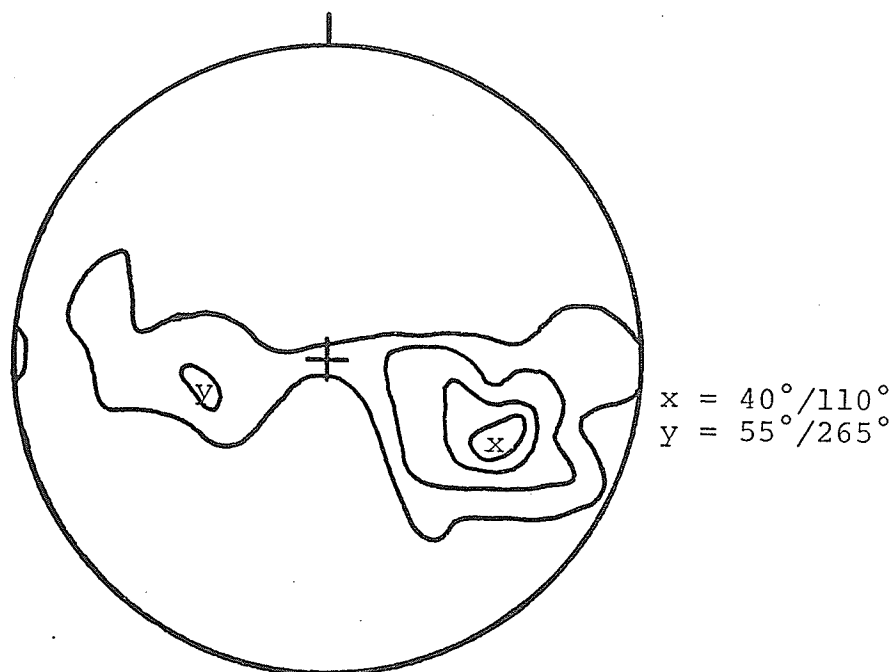


Figure 29. Lower hemisphere, equal-area stereogram of sub-area III. Fold axes (f_4), 58 points, contours 1%, 5% 13%, 17%.

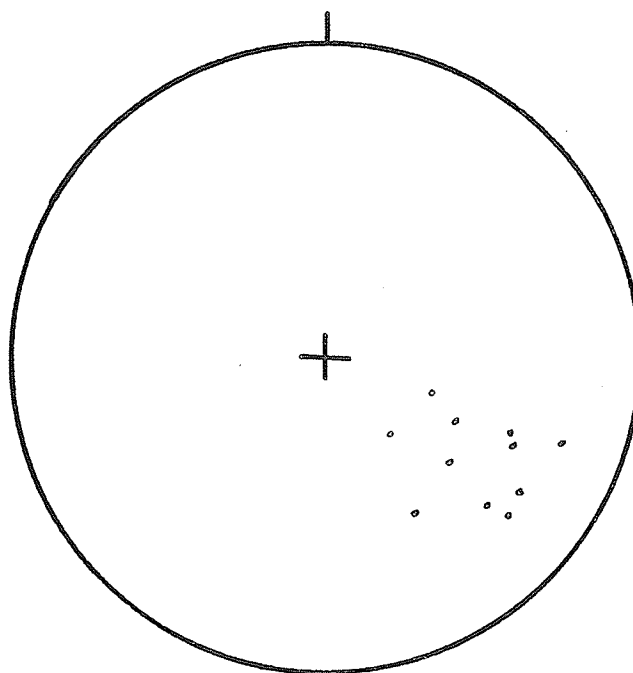


Figure 30. Lower hemisphere, equal-area stereogram of sub-area III. Mineral lineations (m_4), 11 points.

attitudes of the fold axes and that of the linear structures (Figs. 30, 31, 32).

Discussion

The orientation of the fold axes at $40^\circ/110^\circ$ suggests that the rocks were folded about this axis during the fourth deformational event. A similar orientation of m_4 , c_4 , and l_4 suggests that these linear elements were formed during the same deformational event. The minor concentration of westerly-plunging kink folds may represent earlier f_2 folds that have been largely destroyed during subsequent deformation.

Strain Analysis

Folding Mechanism

Evidence which suggests that the folding mechanism was flexural slip, identical to the folding during D_2 is as follows:

1. The layer thickness remains constant in right section.
2. Axial planes to f_4 bisect the interlimb angle.
3. Linear structures parallel the statistical fold axis.

Tectonic Directions

The b kinematic direction is parallel to the statistical fold axis. The a-c plane is perpendicular to this, striking north and dipping 50° W. The kinematic a direction varies in the a-c plane according to the attitude of the

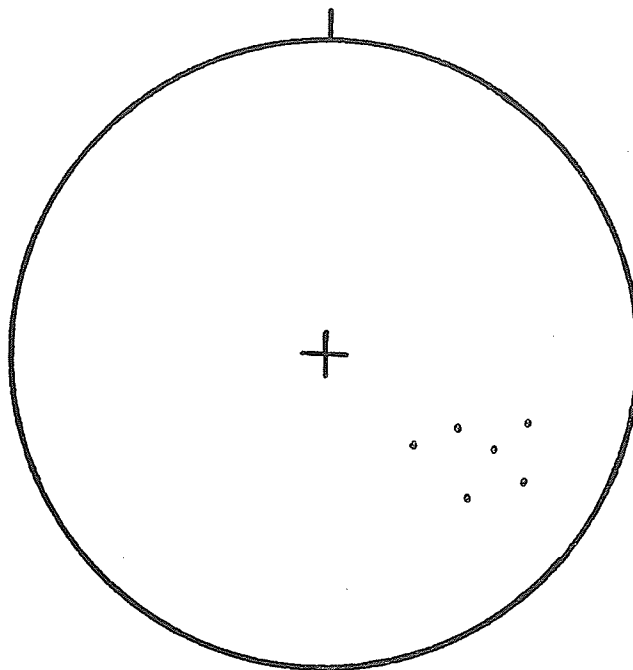


Figure 31. Lower hemisphere, equal-area stereogram of sub-area III. Microcrenulations (c_4), 6 points.

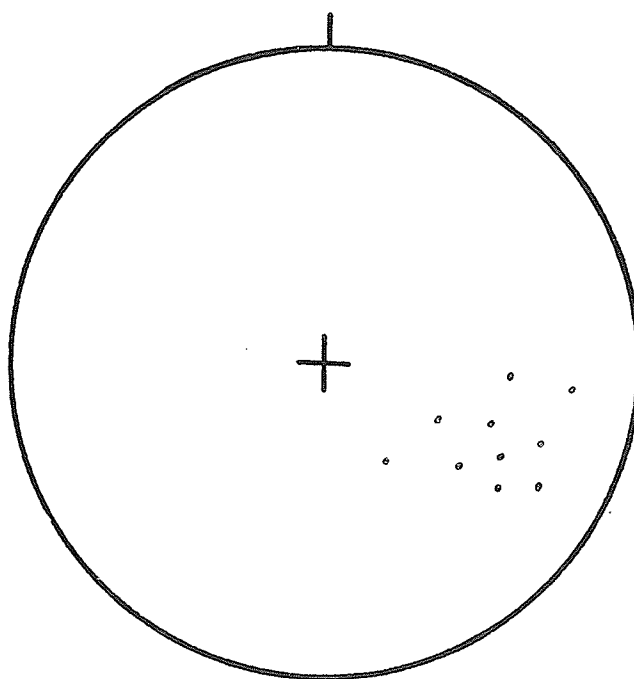


Figure 32. Lower hemisphere, equal-area stereogram of sub-area III. Deformed fragments (l_4), 10 points.

limbs on various parts of the fold. The geometry of the folds suggests shortening in an east-west direction perpendicular to the f_4 plunge direction.

Origin of Linear Structures

Microcrenulations (c_4), mineral lineations (m_4), and the long axes of deformed fragments (l_4) are parallel to the f_4 statistical fold axis in sub-area III. The microcrenulations (c_4) are the small-scale equivalents of the f_4 kink folds. The mineral lineations may represent an earlier lineation reoriented during D_4 , or the development of a new lineation by recrystallization during D_4 . The deformed fragments (l_4) are parallel to the f_4 fold axes and may be reoriented l_1 lineations. Although the origin of m_4 and l_4 is not fully understood, these linear structures have been assigned to the fourth deformational event because they are parallel to the f_4 fold axes.

CHAPTER IX

THE FIFTH DEFORMATIONAL EVENT

The final deformational event is represented by minor faults. Displacements along fault planes are never more than 20 centimetres. Limited orientation data prevent a statistical analysis; however, the faults generally strike NNE and NNW, and are steeply dipping. Both left and right lateral movement is common. The faults displace s_0 , s_1 , and s_1' as well as the limbs of f_4 , f_3 , and f_2 .

CHAPTER X

CONCLUSIONS

At Gods Lake Narrows, Manitoba, the greenstone belt can be divided into two specific stratigraphic subdivisions: the Gods Lake Subgroup and the overlying Oxford Lake Subgroup. The Oxford Lake Subgroup, which is the object of this study, is separated from the Gods Lake Subgroup by a fault contact and is composed largely of volcanogenic metasedimentary rocks.

Detailed mapping has revealed that the Oxford Lake Subgroup has undergone a complex structural history. An analysis of fold styles and the attitudes of s-surfaces and linear structures indicates that there were five periods of deformation including one major period of folding, three minor periods of folding, and one period of faulting.

During the first period of deformation, the rocks of the Oxford Lake Subgroup were folded into a series of large-scale isoclinal folds that presently trend to the southeast and are overturned to the southwest. During this folding event, small-scale shear folds were formed in the bedding by discrete displacements along a penetrative foliation which developed parallel to the axial planes of

these isoclinal folds.

The mechanism of deformation during the first period of folding was probably a combination of pure and simple shear resulting in passive slip on the foliation planes.

Mineral lineations and the long axes of deformed fragments lie in the plane of the foliation and plunge about 65° south. The deformed fragments are also flattened in the plane of the foliation. These linear structures are interpreted to be parallel to the extensive component of first generation strain which lies in the plane of the foliation and which caused passive folding of the bedding. Compressive strain of the rock mass took place in a direction perpendicular to s_1 .

During the second deformational event, the penetrative foliation developed during D_1 was kink folded. Small, westerly-plunging kink folds with z asymmetry were developed during this event. Mineral lineations and microcrenulations are parallel to the fold axes. The mechanism of deformation was flexural slip on the foliation (s_1). The flexural slip took place in a direction perpendicular to the plunge of the f_2 folds, producing an east-west component of shortening.

The third period of deformation was a relatively minor period of symmetrical folding. These folds deform the foliation produced during D_1 as well as the axial planes of f_2 . The folding mechanism was flexural slip on the foliation (s_1). The flexural slip took place perpendicular

to the fold axes with a vertical component of shortening.

The fourth deformational event was another minor period of kink folding. These kink folds have a z asymmetry and plunge east. The folds deform s_1 but their relationship to f_2 and f_3 is not fully understood. Mineral lineations, the long axes of deformed fragments, and micro-crenulations developed parallel to the fold axes. The mechanism of folding was flexural slip on the s_1 foliation. The slip took place perpendicular to the fold axis with an east-west component of shortening.

The final period of deformation was minor faulting which displaces all of the earlier structural elements.

SELECTED REFERENCES

- Barry, G.S.
1961. Geology of the Gods Narrows Area. Manitoba Mines Branch, Publication 60-1.
- Campbell, F.H.A., Elbers, S.J., Gilbert, H.P.
1972. Stratigraphy of the Hayes River Group. Manitoba Mines Branch, Publication 1972-1.
- Donath, F.H., Parker, R.B.
1964. Folds and folding. Bull. Geol. Soc. Am., v. 75, pp. 45-62.
- Hills, E.S.
1963. Elements of Structural Geology. John Wiley and Sons Inc., New York.
- Quinn, H.A.
1961. Oxford House Manitoba. Geol. Surv. Canada, Map 21-1961.
- Wright, J.F.
1931. Oxford House Area, Manitoba. Geol. Surv. Canada, Summ. Rept., Pt. C.

LEGEND

POST OXFORD INTRUSIVE ROCKS



GABBRO



GNEISSIC GRANODIORITE

INTRUSIVE CONTACT

OXFORD LAKE SUBGROUP



PARAGNEISS



ACID CRYSTAL TUFF



VOLCANIC PEBBLE CONGLOMERATE



IRON FORMATION



FRAGMENTAL HORNBLLENDE GREYWACKE



GARNETIFEROUS AMPHIBOLITE



AMPHIBOLITE



BASIC VOLCANIC BRECCIA



PILLOW BASALT



HORNBLLENDE GREYWACKE



VOLCANIC BOULDER CONGLOMERATE

FAULT CONTACT

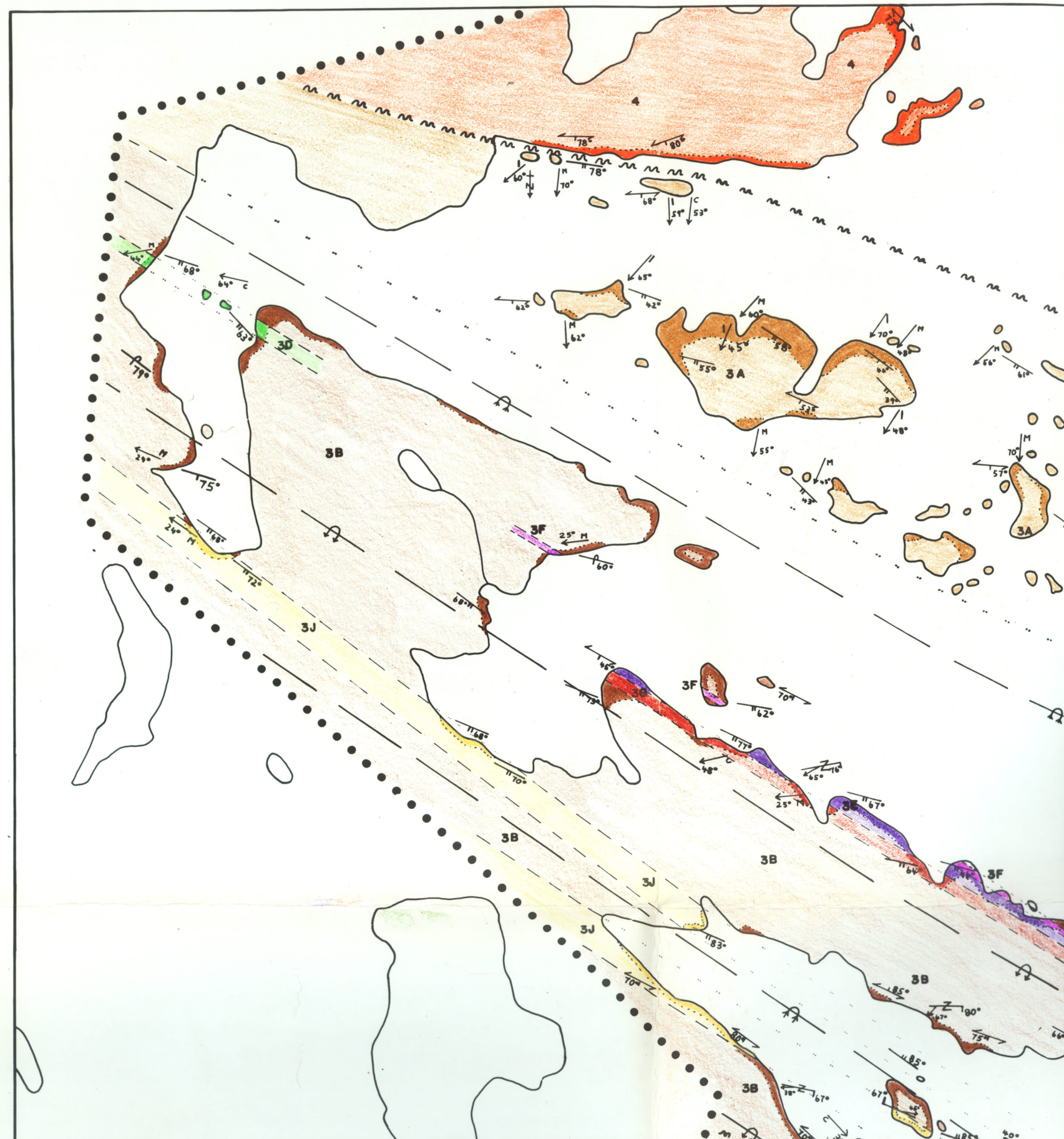
GODS LAKE SUBGROUP



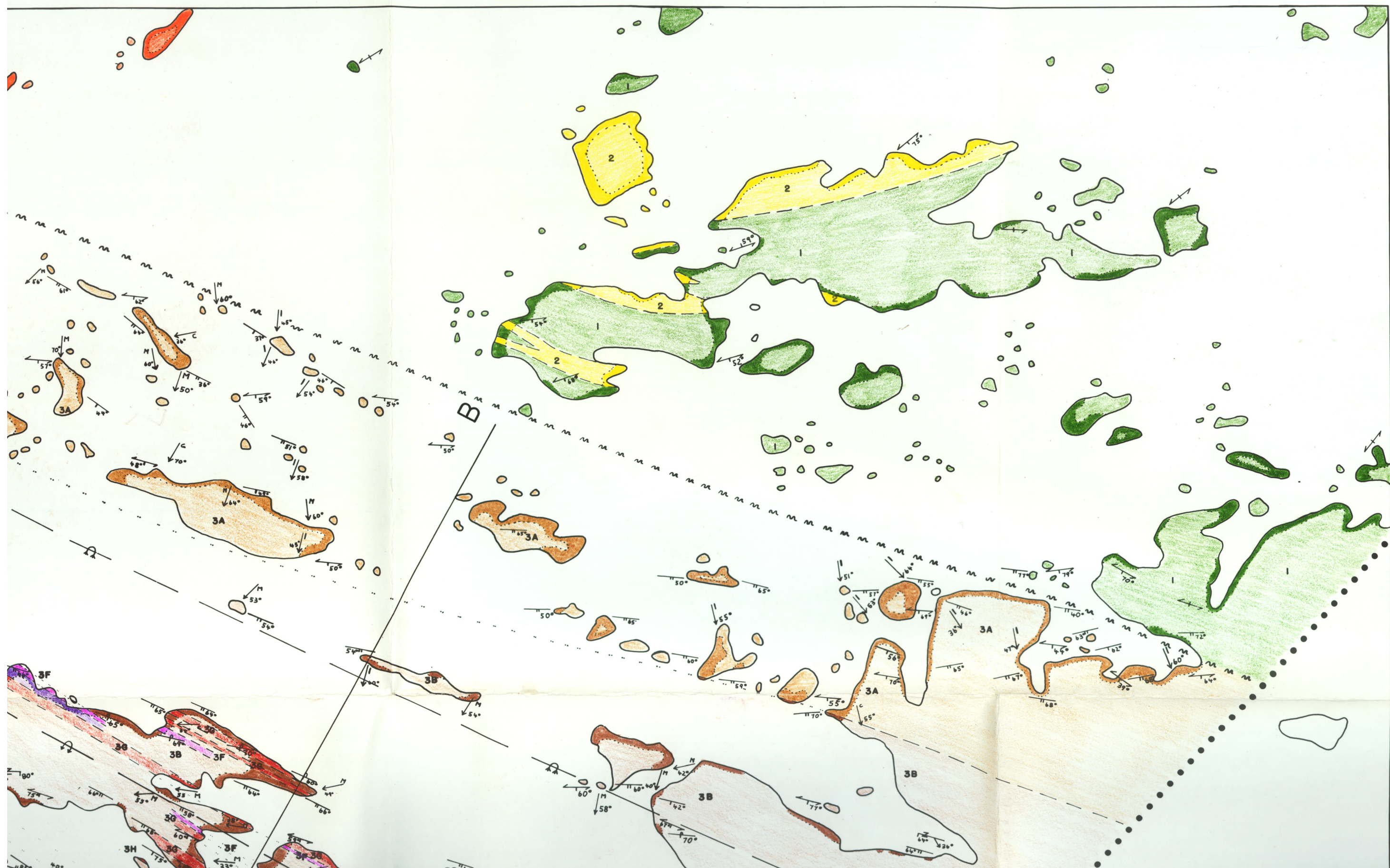
QUARTZ CRYSTAL TUFF

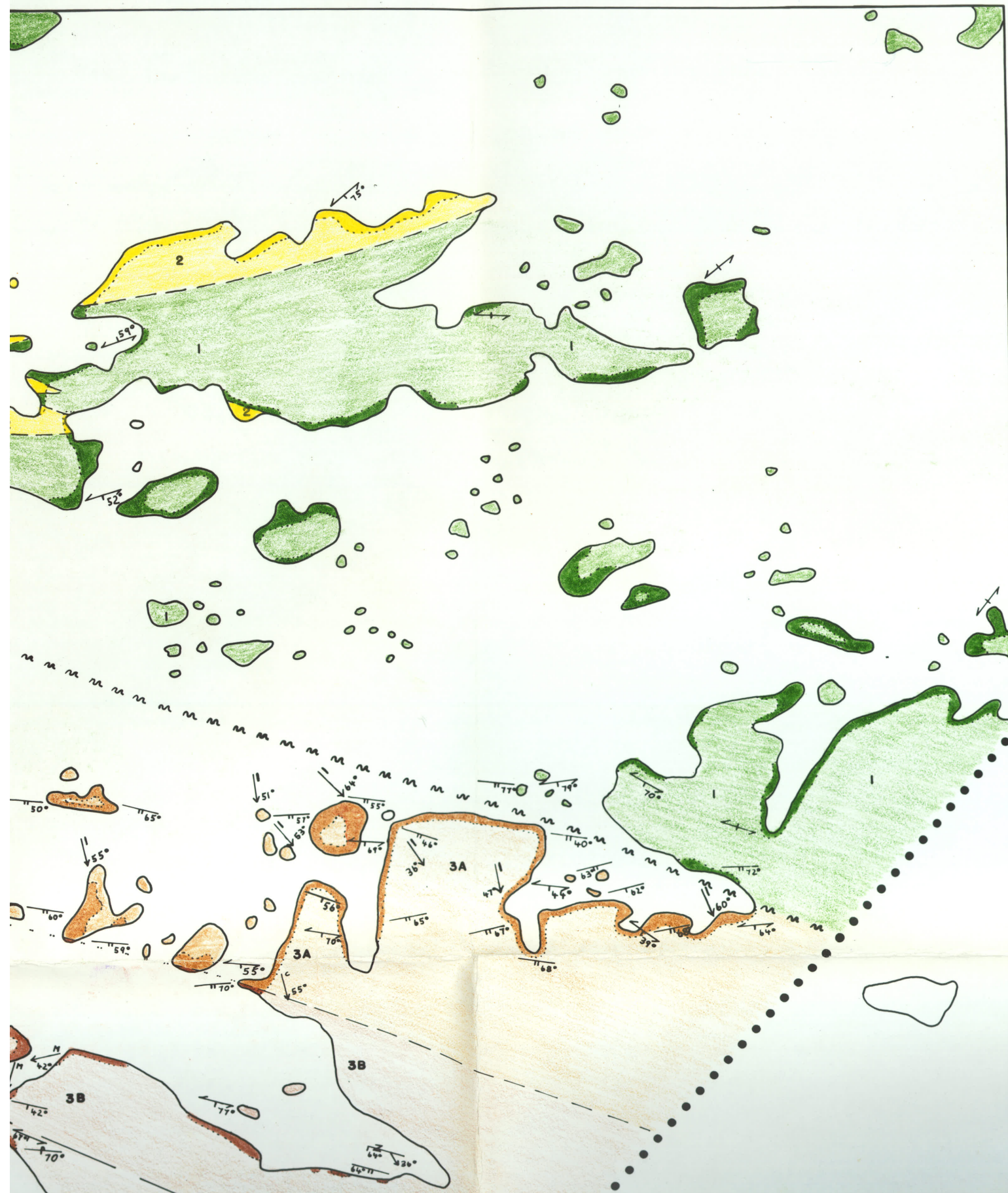


UNDIFFERENTIATED ANDESITE AND BASALT



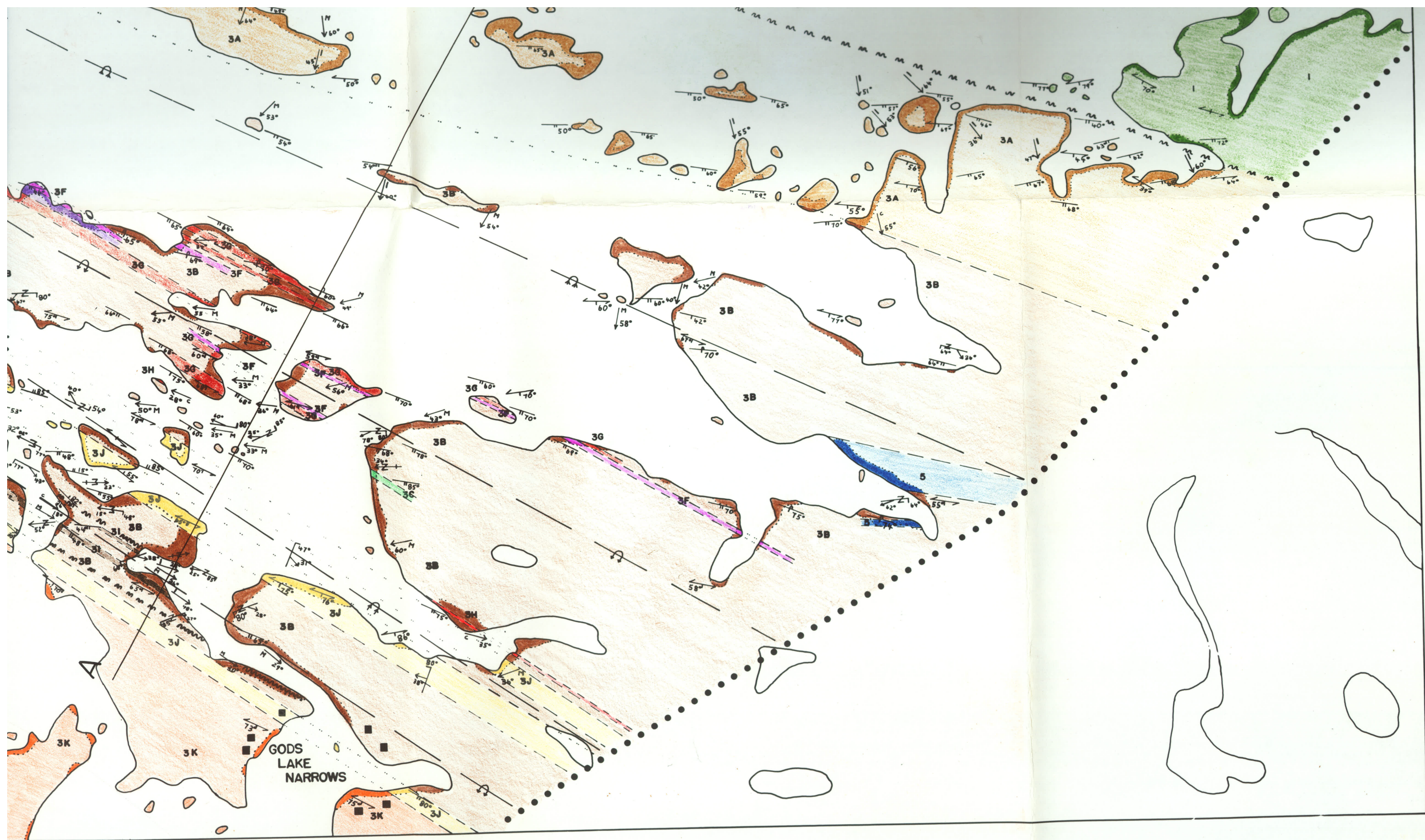
THE UNIVERSITY
OF MANITOBA
ELIZABETH DAFOE LIBRARY





SYMBOLS

	AREA OF ROCK EXPOSURE
	GEOLOGICAL BOUNDARY (DEFINED, APPROXIMATE, UNDERWATER)
LAYERING 	BEDDING, TOPS KNOWN (INCLINED, VERTICAL, OVERTURNED)
	BEDDING, TOPS UNKNOWN (INCLINED, VERTICAL)
	PILLOW TOP DIRECTIONS (INCLINED, VERTICAL, OVERTURNED)
FOLIATION 	SCHISTOSITY (INCLINED, VERTICAL, DIP UNKNOWN)
MAJOR FOLDS 	ANTICLINE, OVERTURNED
	SYNCLINE, OVERTURNED
MINOR FOLDS 	AXES (HORIZONTAL, INCLINED)
	AXIAL PLANE (HORIZONTAL, INCLINED, VERTICAL)
	SYMMETRY (ASYMMETRICAL Z SHAPED, SYMMETRICAL)
LINEAR STRUCTURES 	MINERAL LINEATIONS (HORIZONTAL, INCLINED)
	MICROCRENULATIONS (HORIZONTAL, INCLINED)
	DEFORMED FRAGMENTS (HORIZONTAL, INCLINED)
FAULTS, SHEARED ZONES 	FAULTS, SHEARED ZONES (DEFINED, APPROXIMATE)
	CABIN
	LIMIT OF MAPPING



GEOLOGY OF THE GODS LAKE
NARROWS AREA

